Bonn-Gatchina partial wave analysis

A. Sarantsev

HISKP, Uni-Bonn (Bonn) and PNPI (Gatchina)

N*- resonances in the quark model

Nukleon

10^{-15} m

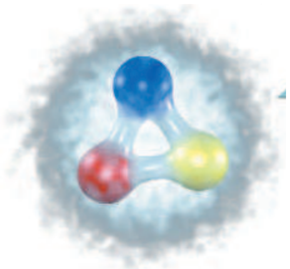

U. Loering, B. Metsch, H. Petry et al. (Bonn)

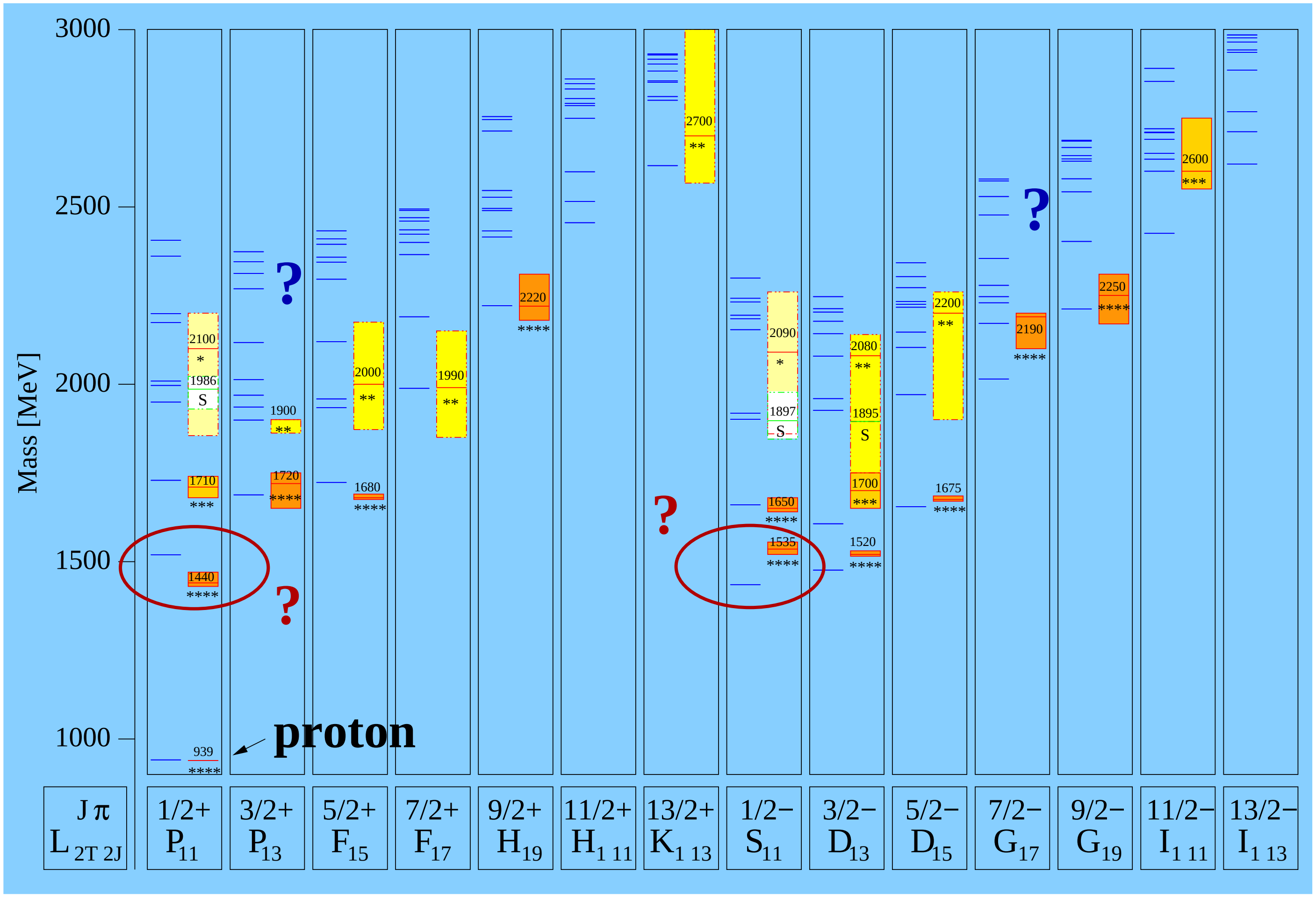

↔

Constituent quarks

Confinement-potential

Residual interaction

The Δ^*- states

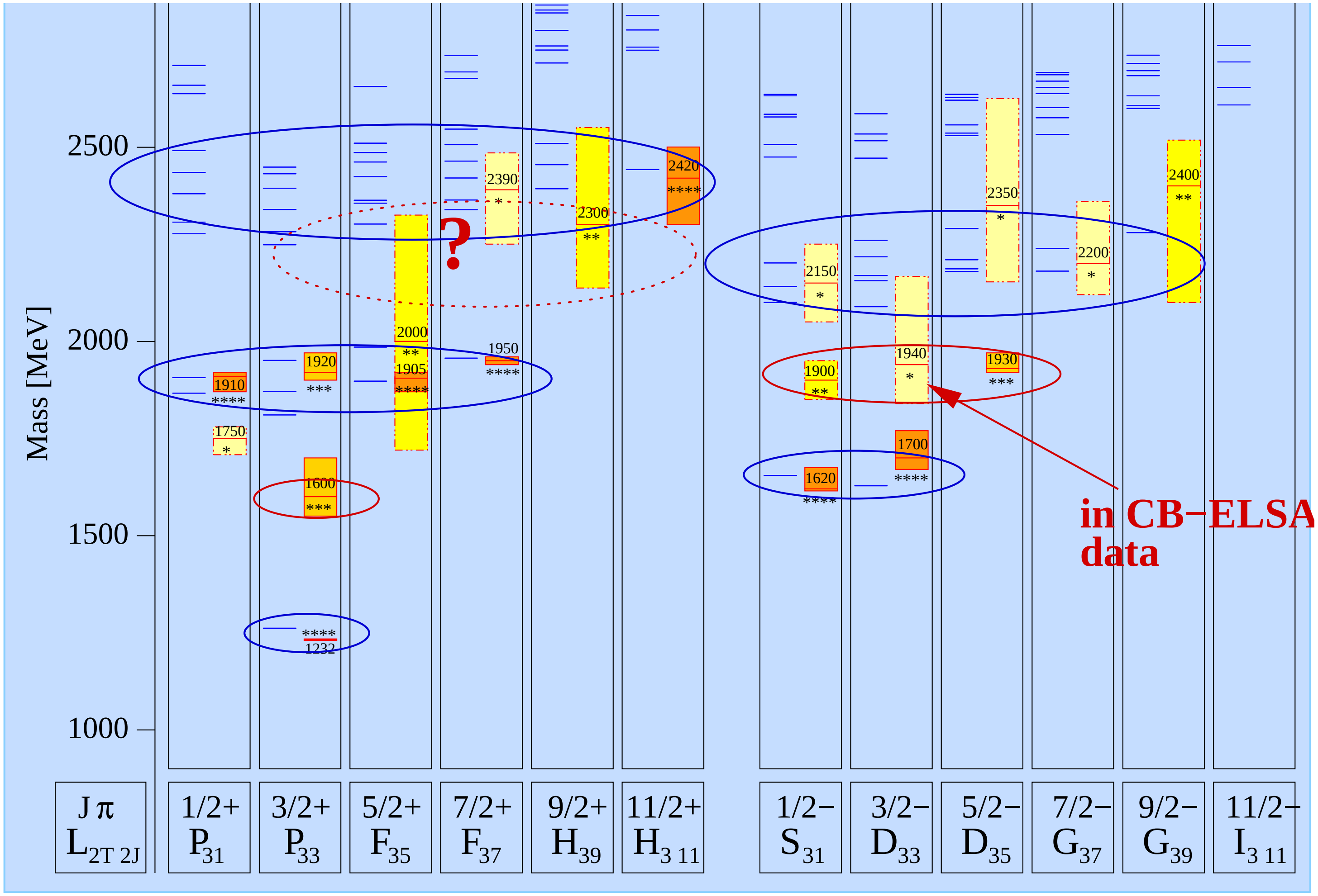

Quark model
U. Löring, B. Metsch, H. Petry et al.

model
$\sim 2n + \ell$

data
$\sim n + \ell$?

$\leftrightarrow$ **Parity doublets ?**

$\Leftrightarrow$ **Additional experimental information needed !!**

Problems in the baryon spectroscopy and/or quark model:

1. **Problem: The number of predicted three quark states exceeds dramatically the number of discovered baryons.**

2. **Possible solution: Most of the information comes from the analysis of meson induced reactions and meson-baryon final states. Photoproduction data taken by CLAS, GRAAL, LEPS and CB-ELSA can provide an important information about missing states.**

   (a) **problem: The unambiguous analysis of photoproduction reactions can not be done without polarization information available.**

   (b) **problem: Signals in simple reactions are expected to be mostly weak. Strong signals from new resonances can be found in multi-meson final states.**

   (c) **Possible solution 1: The single polarization observables are measured now by almost all collaborations. In the nearest future single and double polarization data will be available from CLAS and CB-ELSA.**

   (d) **Possible solution 2: A combined analysis of the large data sets.**

The fitted reactions. Recently included data sets. New points added

Observable	$N_{\rm data}$	$\frac{\chi^2}{N_{\rm data}}$		Observable	$N_{\rm data}$	$\frac{\chi^2}{N_{\rm data}}$	
$\sigma(\gamma p \to p\pi^0)$	1106	1.27	CB-ELSA	$\sigma(\gamma p \to p\pi^0)$	861	1.74	GRAAL
$\sigma(\frac{3}{2}-\frac{1}{2})(p\pi^0)$	140	1.41	A2GDH	$\Sigma(\gamma p \to p\pi^0)$	1492	3.38	SAID
$P(\gamma p \to p\pi^0)$	607	3.16	SAID	$T(\gamma p \to p\pi^0)$	389	4.01	SAID
$H(\gamma p \to p\pi^0)$	71	1.92	SAID	$G(\gamma p \to p\pi^0)$	75	2.58	SAID
$Ox(\gamma p \to p\pi^0)$	7	1.01	SAID	$Oz(\gamma p \to p\pi^0)$	7	0.38	SAID
$\sigma(\gamma p \to n\pi^+)$	1583	1.87	SAID	$\sigma(\gamma p \to n\pi^+)$	408	2.09	A2GDH
$\Sigma(\gamma p \to n\pi^+)$	899	4.23	SAID	$\sigma(\frac{3}{2}-\frac{1}{2})(n\pi^+)$	231	2.49	A2GDH
$P(\gamma p \to n\pi^+)$	252	3.90	SAID	$T(\gamma p \to n\pi^+)$	661	3.66	SAID
$H(\gamma p \to p\pi^0)$	71	1.92	SAID	$G(\gamma p \to p\pi^0)$	75	2.58	SAID
$S_{11}(\pi N \to \pi N)$	126	1.40	SAID	$P_{11}(\pi N \to \pi N)$	110	2.24	SAID
$P_{13}(\pi N \to \pi N)$	108	2.57	SAID	$P_{33}(\pi N \to \pi N)$	130	5.01	SAID
$D_{33}(\pi N \to \pi N)$	136	4.01	SAID				
$\sigma(\gamma p \to p\eta)$	667	0.92	CB-ELSA	$\sigma(\gamma p \to p\eta)$	100	2.72	TAPS
$\Sigma(\gamma p \to p\eta)$	51	2.06	GRAAL 98	$\Sigma(\gamma p \to p\eta)$	100	2.01	GRAAL 04
$T(\gamma p \to p\eta)$	50	1.52	Phoenics	$\sigma(\pi^- p \to n\eta)$	288	2.76	CBALL+Richards

The fitted reactions. Recently included data sets.

Observable	$N_{\rm data}$	$\frac{\chi^2}{N_{\rm data}}$		Observable	$N_{\rm data}$	$\frac{\chi^2}{N_{\rm data}}$	
$C_x(\gamma p \to \Lambda K^+)$	160	1.22	CLAS	$C_x(\gamma p \to \Sigma^0 K^+)$	94	2.29	CLAS
$C_z(\gamma p \to \Lambda K^+)$	160	1.53	CLAS	$C_z(\gamma p \to \Sigma^0 K^+)$	94	2.19	CLAS
$\sigma(\gamma p \to \Lambda K^+)$	1377	1.70	CLAS	$\sigma(\gamma p \to \Sigma^0 K^+)$	1280	1.95	CLAS
$P(\gamma p \to \Lambda K^+)$	202	2.23	CLAS	$P(\gamma p \to \Sigma^0 K^+)$	95	1.56	CLAS
$\Sigma(\gamma p \to \Lambda K^+)$	66	2.11	GRAAL	$\Sigma(\gamma p \to \Sigma^0 K^+)$	42	0.67	GRAAL
$\Sigma(\gamma p \to \Lambda K^+)$	45	1.75	LEP	$\Sigma(\gamma p \to \Sigma^0 K^+)$	45	1.03	LEP
$T(\gamma p \to \Lambda K^+)$	66	2.11	GRAAL	$\sigma(\gamma p \to \Sigma^+ K^0)$	48	3.36	CLAS
$Ox(\gamma p \to \Lambda K^+)$	66	1.40	GRAAL	$\sigma(\gamma p \to \Sigma^+ K^0)$	160	0.95	CB-ELSA
$Oz(\gamma p \to \Lambda K^+)$	66	1.86	GRAAL	$P(\gamma p \to \Sigma^+ K^0)$	72	0.72	CB-ELSA
$\sigma(\gamma p \to p\pi^0\pi^0)$	CB-ELSA (1.4 GeV)			$E(\gamma p \to p\pi^0\pi^0)$	16	2.08	MAMI
$\sigma(\gamma p \to p\pi^0\eta)$	CB-ELSA (3.2 GeV)			$\Sigma(\gamma p \to p\pi^0\eta)$	180	2.68	GRAAL
$\sigma(\gamma p \to p\pi^0\pi^0)$	CB-ELSA (3.2 GeV)			$\Sigma(\gamma p \to p\pi^0\pi^0)$	128	0.85	GRAAL

Combined analysis of the different reactions:

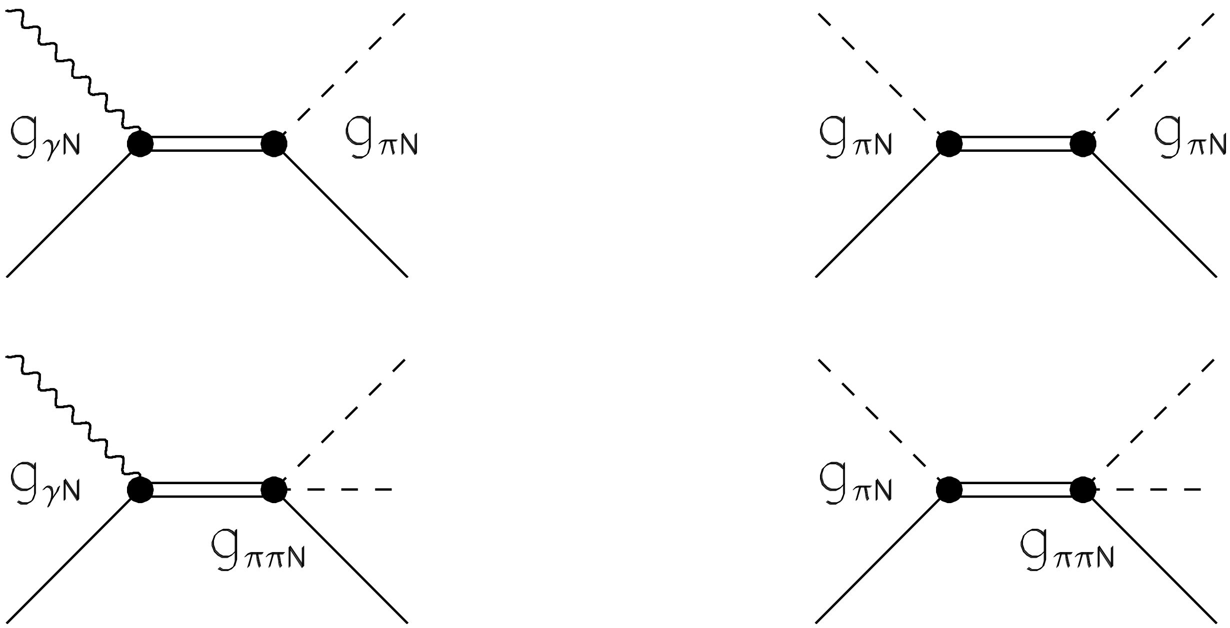

$$BW = \frac{g_i g_j}{M^2 - s - i\sum_k g_k^2 \rho_k}, \qquad g_k = g_{\pi N}, g_{\gamma N}, g_{\pi\pi N}, \ldots$$

$$M\Gamma = \sum_k g_k^2 \rho_k$$

The resonance amplitudes for meson photoproduction

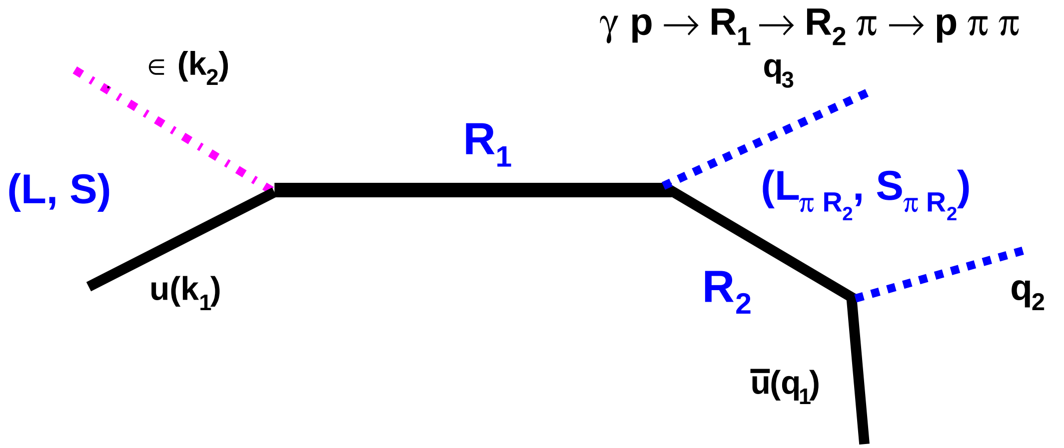

The general form of the angular dependent part of the amplitude:

$$\bar{u}(q_1)\tilde{N}_{\alpha_1\ldots\alpha_n}(R_2\to\mu N)F^{\alpha_1\ldots\alpha_n}_{\beta_1\ldots\beta_n}(q_1+q_2)\tilde{N}^{(j)\beta_1\ldots\beta_n}_{\gamma_1\ldots\gamma_m}(R_1\to\mu R_2)$$
$$F^{\gamma_1\ldots\gamma_m}_{\xi_1\ldots\xi_m}(P)V^{(i)\mu}_{\xi_1\ldots\xi_m}(R_1\to\gamma N)u(k_1)\varepsilon_\mu$$

$$F^{\mu_1\ldots\mu_L}_{\nu_1\ldots\nu_L}(p)=(m+\hat{p})O^{\mu_1\ldots\mu_L}_{\alpha_1\ldots\alpha_L}\frac{L+1}{2L+1}\left(g^{\perp}_{\alpha_1\beta_1}-\frac{L}{L+1}\sigma_{\alpha_1\beta_1}\right)\prod_{i=2}^{L}g_{\alpha_i\beta_i}O^{\beta_1\ldots\beta_L}_{\nu_1\ldots\nu_L}$$

$$\sigma_{\alpha_i\alpha_j}=\frac{1}{2}(\gamma_{\alpha_i}\gamma_{\alpha_j}-\gamma_{\alpha_j}\gamma_{\alpha_i})$$

The Reggezied $t-$ and $u-$ channel exchanges can be projected to the s-channel.

$$J_\mu = i\mathcal{F}_1\sigma_\mu + \mathcal{F}_2(\vec\sigma\vec q)\frac{\varepsilon_{\mu ij}\sigma_i k_j}{|\vec k||\vec q|} + i\mathcal{F}_3\frac{(\vec\sigma\vec k)}{|\vec k||\vec q|}q_\mu + i\mathcal{F}_4\frac{(\vec\sigma\vec q)}{\vec q^2}q_\mu \ .$$

the multipoles can be reconstructed as:

$$\begin{aligned}
E_n^+ &= \frac{1}{n+1}\int\frac{dz}{2}\ \mathcal{F}_1 P_n(z) - \mathcal{F}_2 P_{n+1}(z) + \mathcal{F}_3\frac{1-z^2}{(n+1)}P'_n(z) + \mathcal{F}_4\frac{1-z^2}{(n+2)}P'_{n+1}(z)\\
M_n^+ &= \frac{1}{n+1}\int\frac{dz}{2}\ \mathcal{F}_1 P_n(z) - \mathcal{F}_2 P_{n+1}(z) - \mathcal{F}_3\frac{1-z^2}{n(n+1)}P'_n(z)\\
E_n^- &= \int\frac{dz}{2}\frac{(n+1)^2(n+2)}{2n+1}\left[-\mathcal{F}_1 P_{n+1}(z) + \mathcal{F}_2 P_n(z)\right] +\\
&\quad \int\frac{dz}{2}\frac{2(2n-1)(1-z^2)}{(2n+1)(2n-3)}\ \mathcal{F}_3 P'_{n+1}(z) + \frac{(n+2)}{n(2n-3)}\mathcal{F}_4 P'_n(z)\\
M_n^- &= \int\frac{dz}{2}\ \frac{(n+1)^2(n+2)}{2n+1}\ \mathcal{F}_1 P_{n+1}(z) - \mathcal{F}_2 P_n(z)\ \ + \frac{(1-z^2)}{(2n+1)}\mathcal{F}_3 P'_{n+1}(z)
\end{aligned}$$

$\gamma p \to \pi^0 p$ from Crystal Barrel at ELSA ($E_\gamma \leq 3.2$ GeV)

$\Delta(1232)P_{33}$
$N(1520)D_{13}\ S_{11}$
$N(1680)F_{15}$
$\Delta(1700)D_{33}$
$\Delta(1920)P_{33}$

Non-resonance contribution:

t-channel $\rho - \omega$ exchange, u-exchange and non-resonance production in $J^P = 3/2^+$ wave

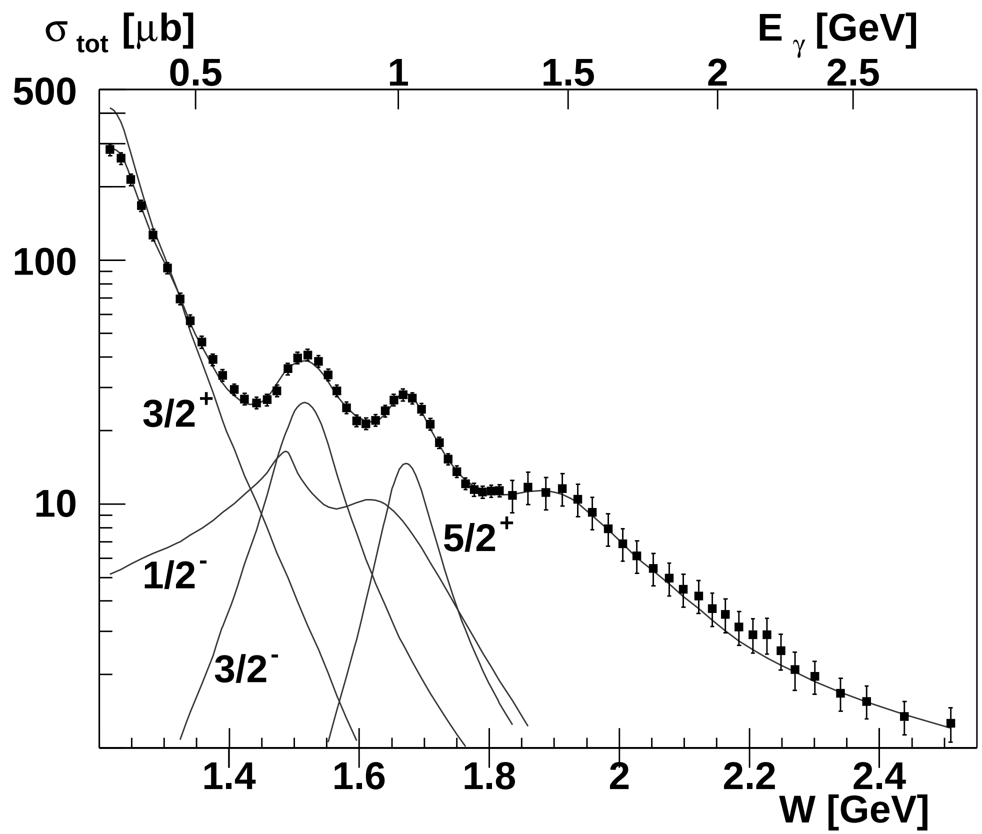

The multipoles for single pion production. Red - real part, Blue - imaginary part. Solid curves BoGa -solution, dashed curves - SAID solution, dotted - MAID 2009.

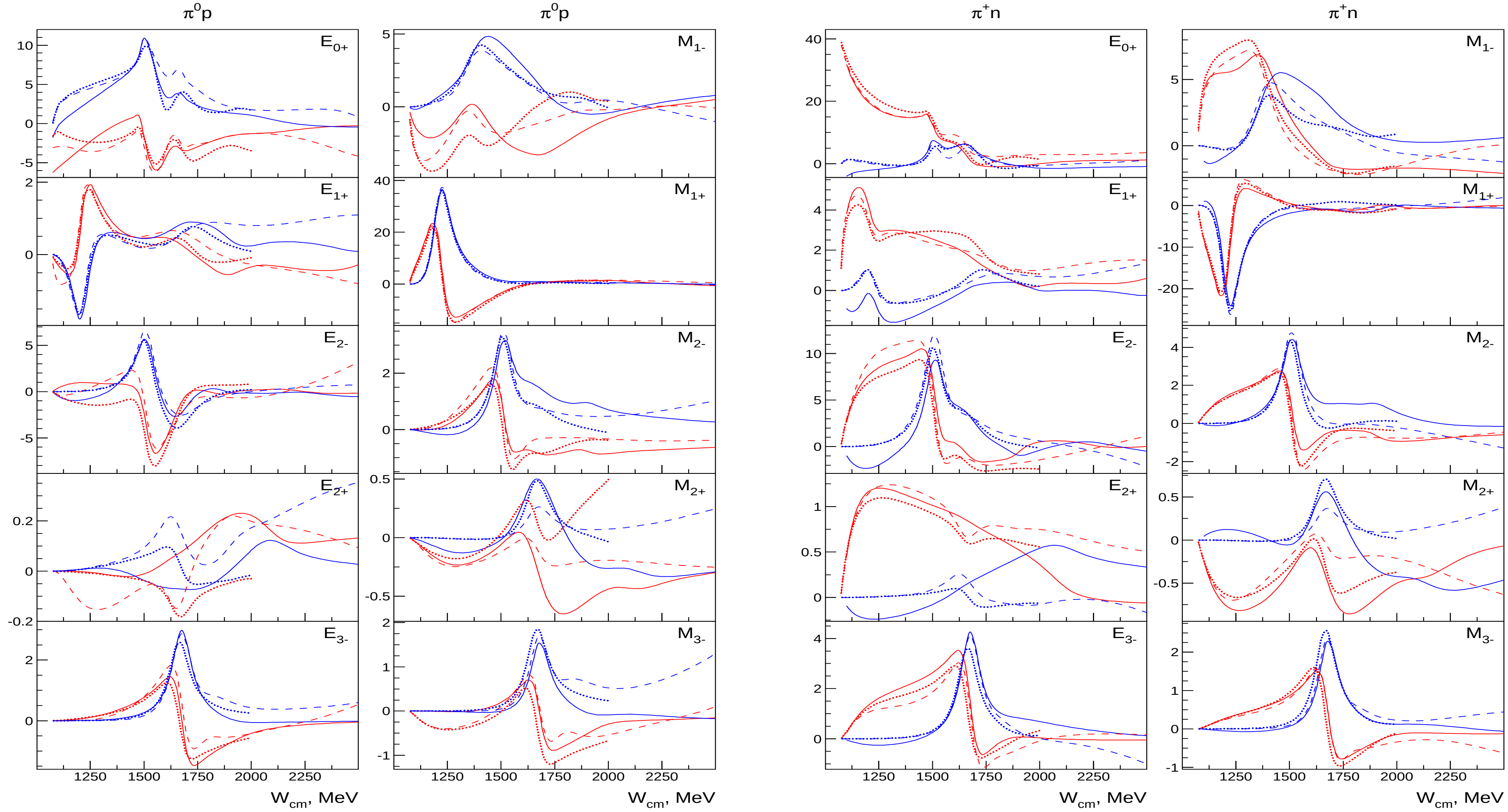

The multipoles for single pion production. Red - real part, Blue - imaginary part. Solid curves solution 1, dashed curves solution 2.

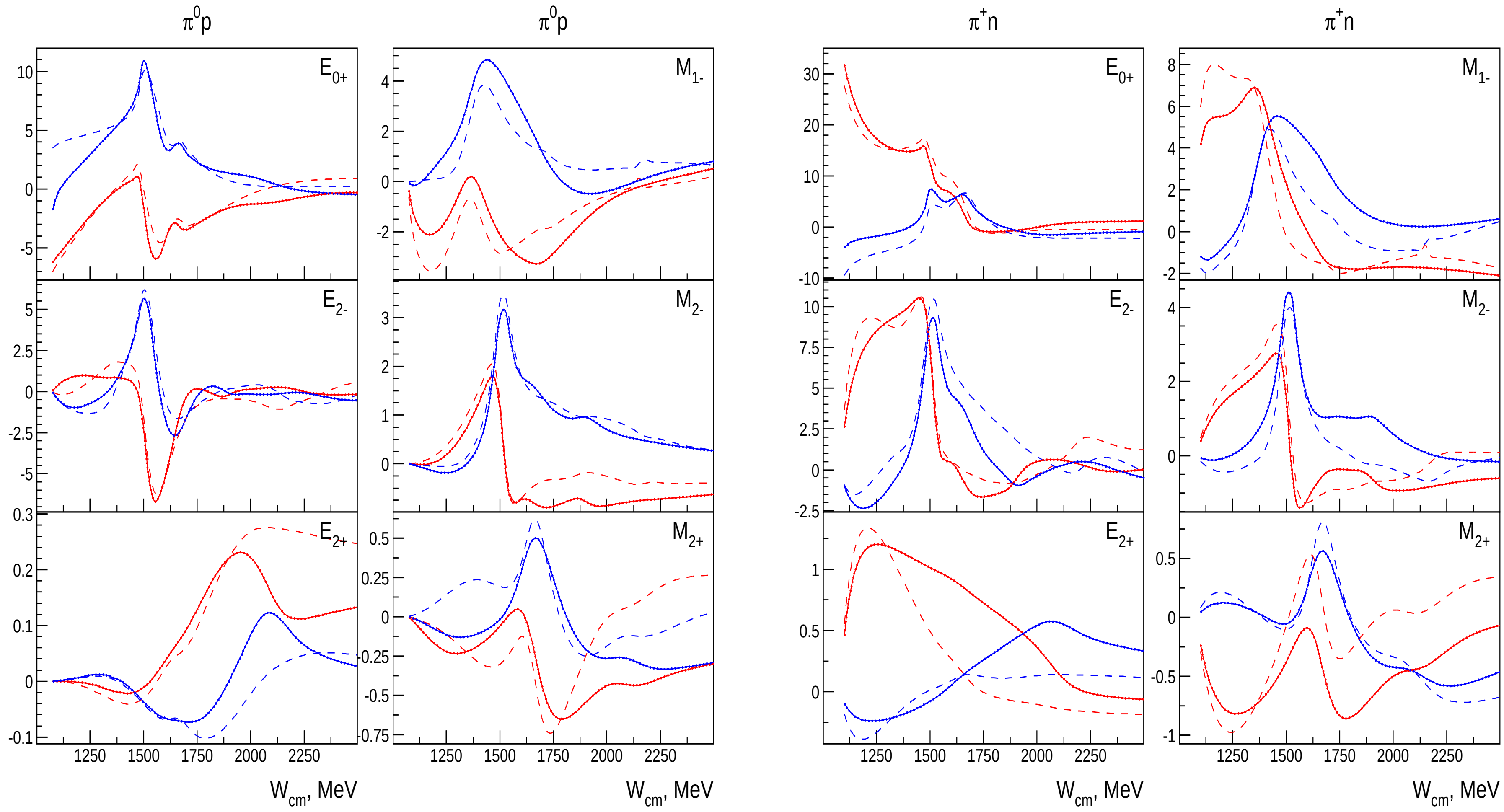

$\gamma p \to \eta p$ from Crystal Barrel at ELSA ($E_\gamma \leq 3.2$ GeV)

Main resonance contributions:

$N(1535)S_{11}$

$N(1650)S_{11}$

$N(1720)P_{13}$

new $N(2070)D_{15}$

Non-resonance contribution: reggezied t-channel $\rho - \omega$ exchange.

No evidence for third $N(1800)S_{11}$

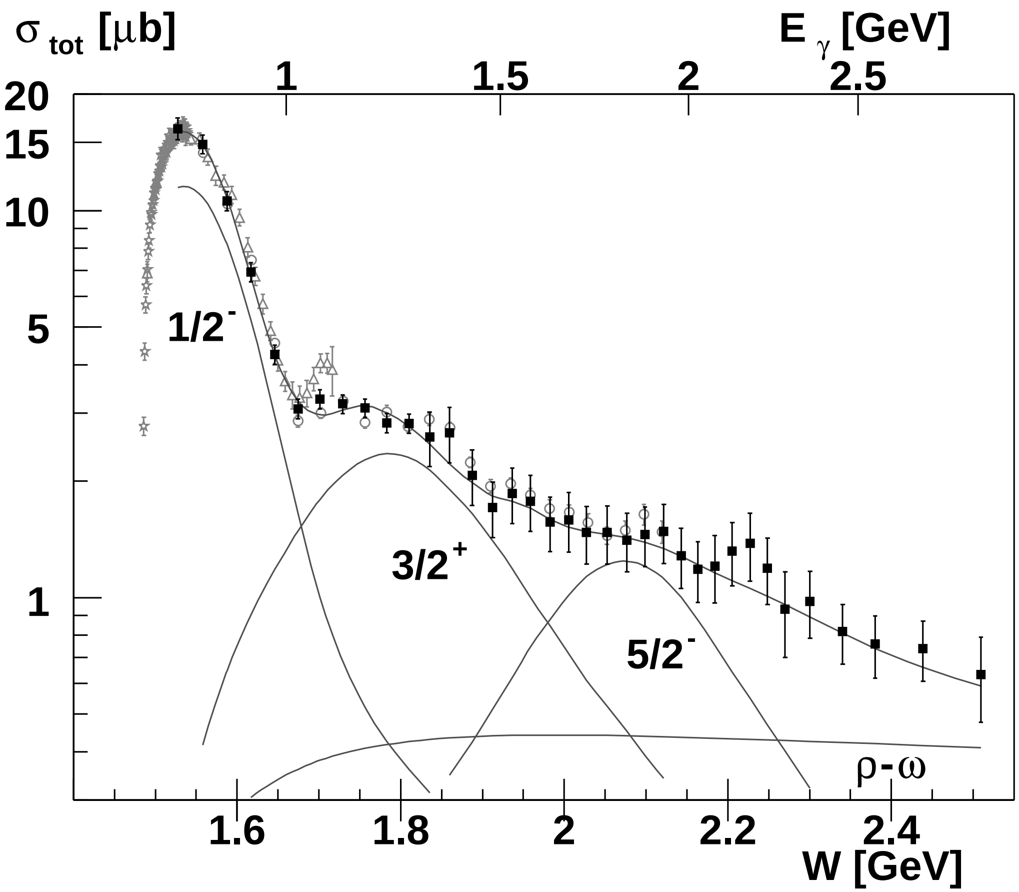

The data on $\pi^- p \to \eta n$ and the target asymmetry $\gamma p \to \eta p$ fix the position and couplings of $P_{11}(1710)$ state and reduce ηN coupling of the $P_{13}(1720)$ state.

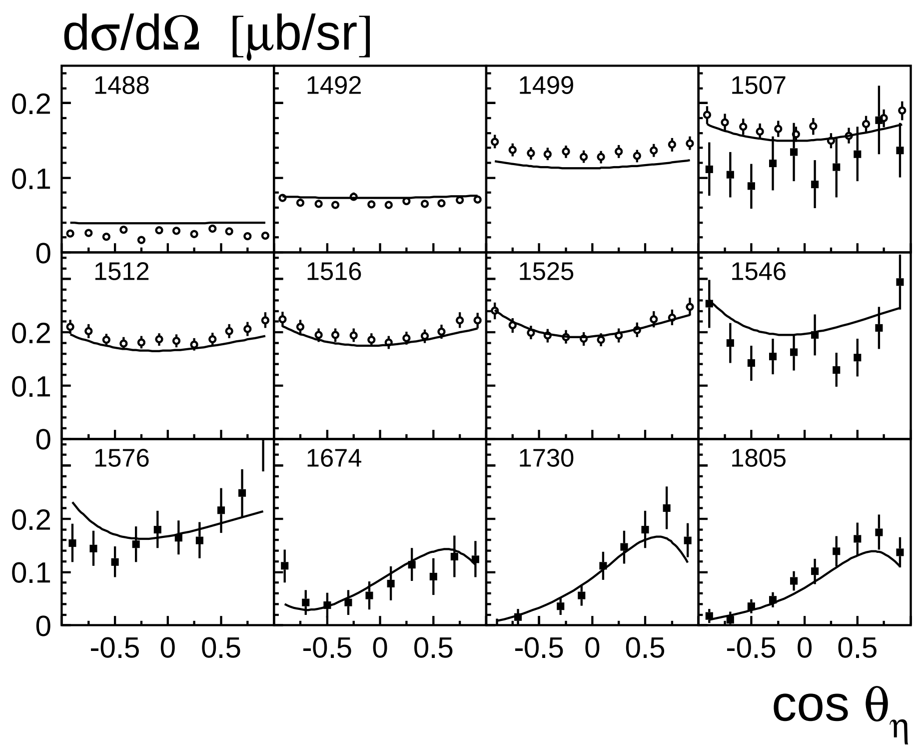

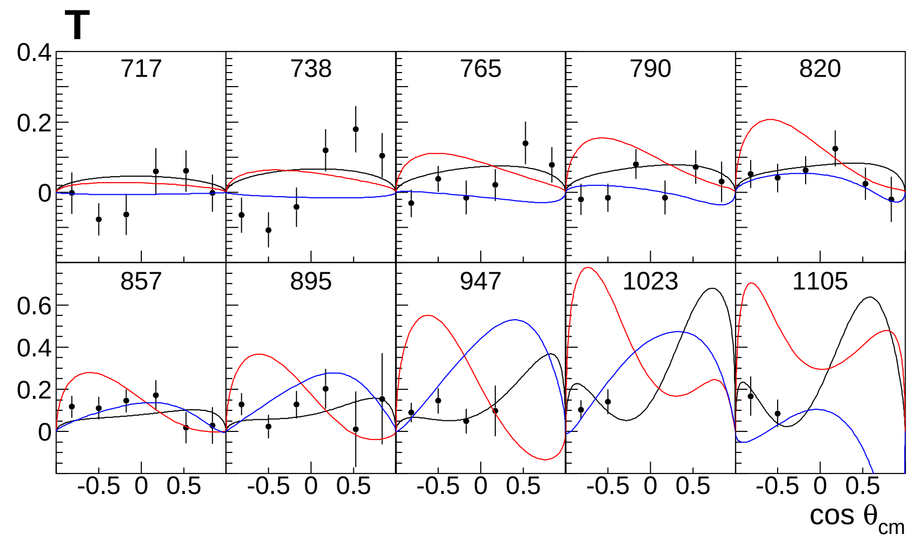

Observable	$N_{\rm data}$	$\frac{\chi^2}{N_{\rm data}}$		Observable	$N_{\rm data}$	$\frac{\chi^2}{N_{\rm data}}$	
$\sigma(\gamma p \to p\eta)$	667	0.92 (0.85)	CB-ELSA	$\sigma(\gamma p \to p\eta)$	100	2.72 (1.97)	TAPS
$\Sigma(\gamma p \to p\eta)$	51	2.06 (1.81)	GRAAL 98	$\Sigma(\gamma p \to p\eta)$	100	2.01 (1.43)	GRAAL 04

$N\pi \to N\pi$ P_{11} wave (3 pole 4 channel K-matrix)

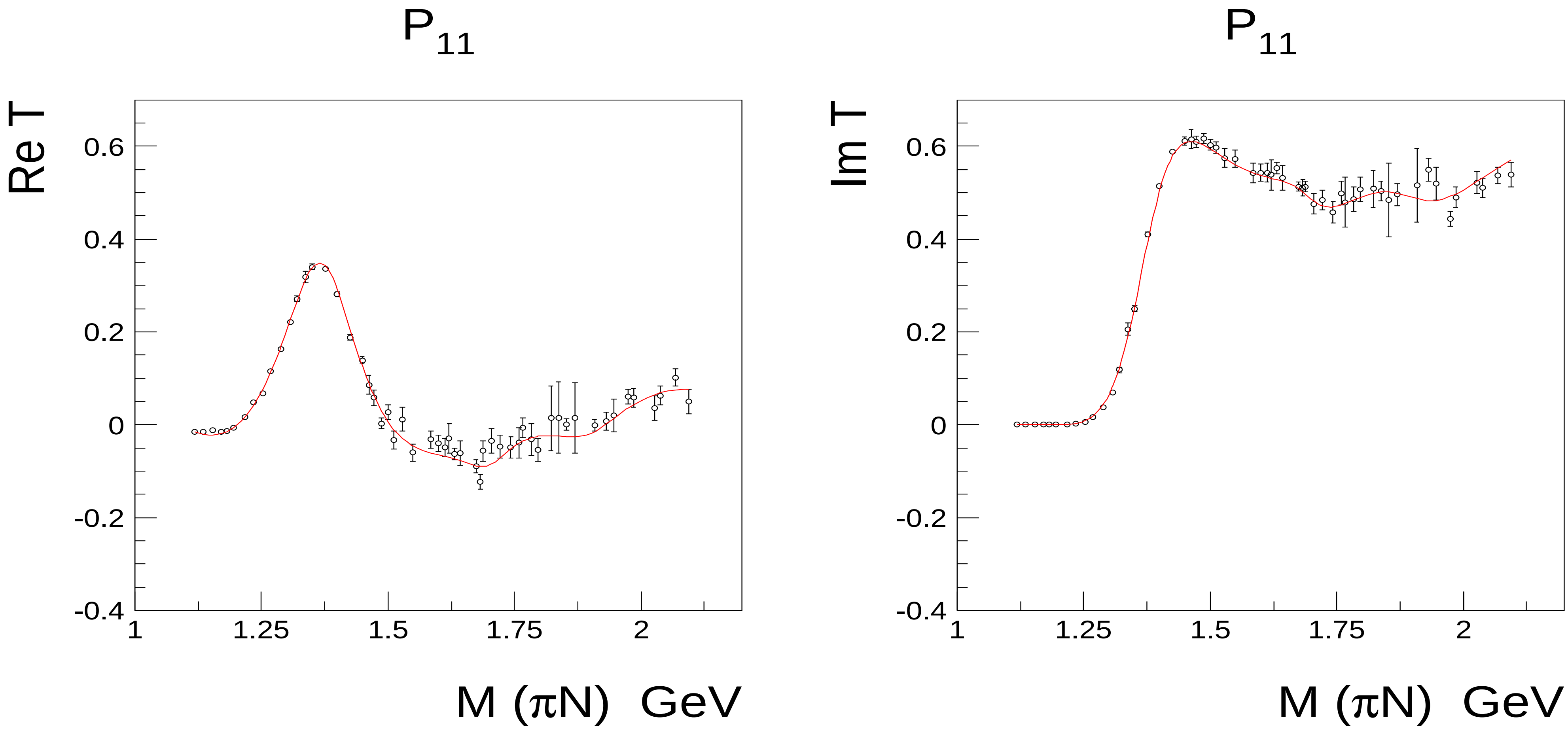

T-matrix poles: $M = 1371 \pm 7$ **MeV,** $2\ Im = 192 \pm 20$ **MeV;**

$M = 1710 \pm 10$ **MeV,** $2\ Im = 160 \pm 50$ **MeV**

$M = 1850 \pm 10$ **MeV,** $2\ Im = 150 \pm 20$ **MeV**

The target asymmetry $\gamma p \to \eta p$ data reduce coupling of the $P_{13}(1720)$ state to the ηN channel by factor $\sim$ 1.7.

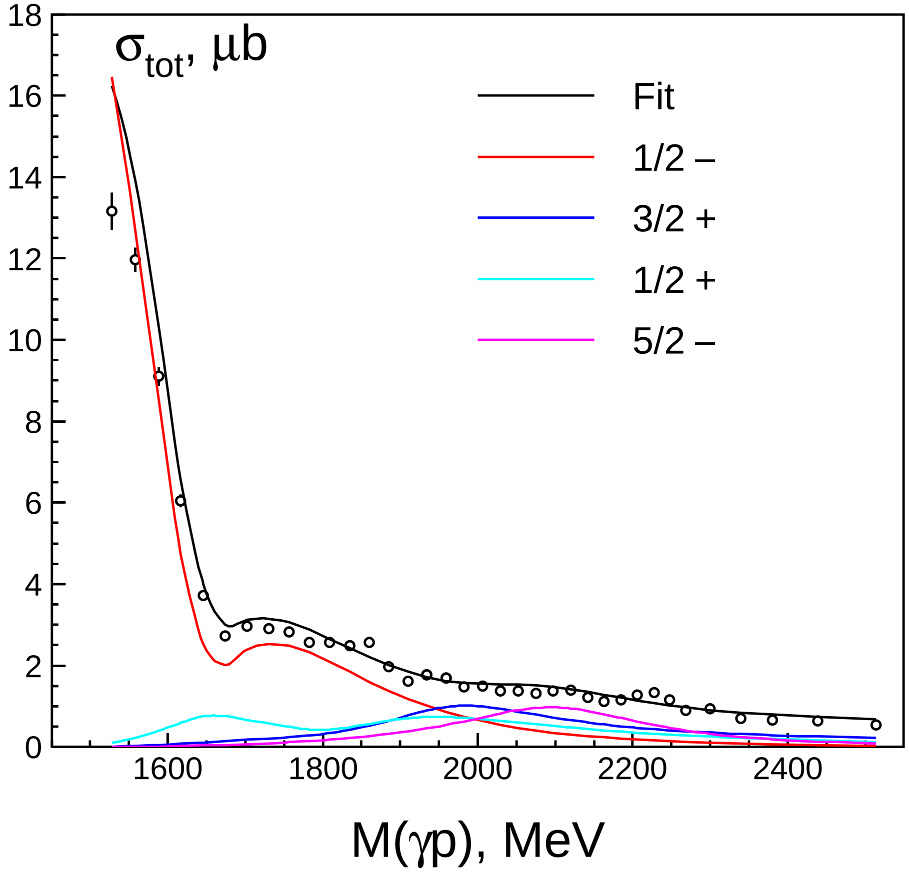

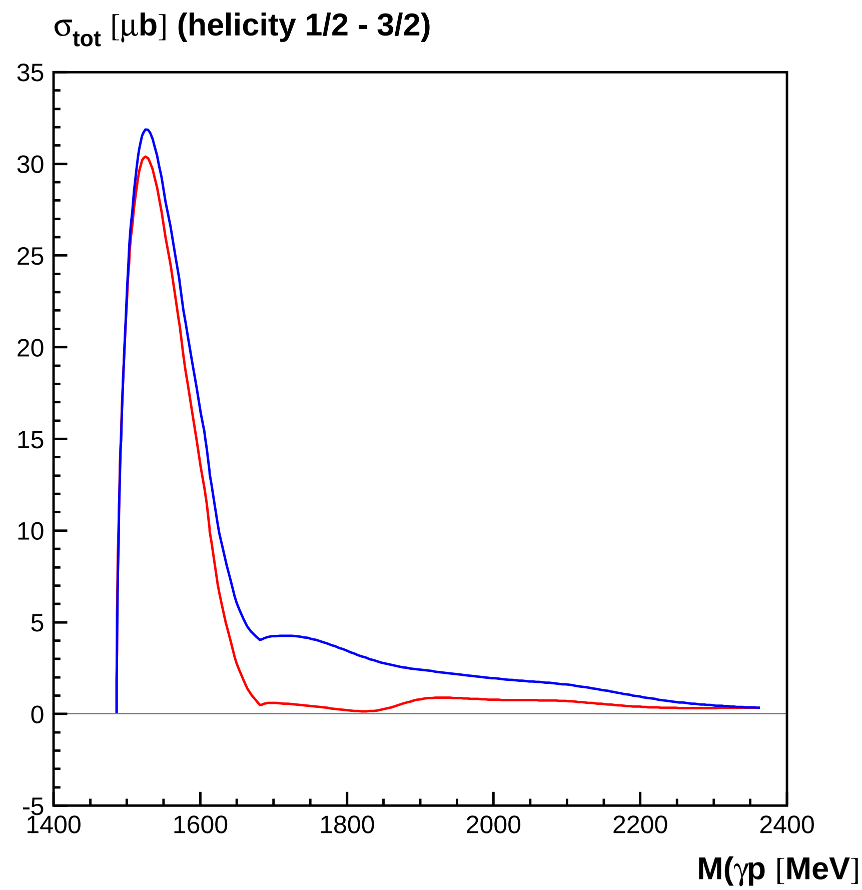

The solution, which explains angular dependence of C_x and C_z observables due to $P_{13}(1900)$:

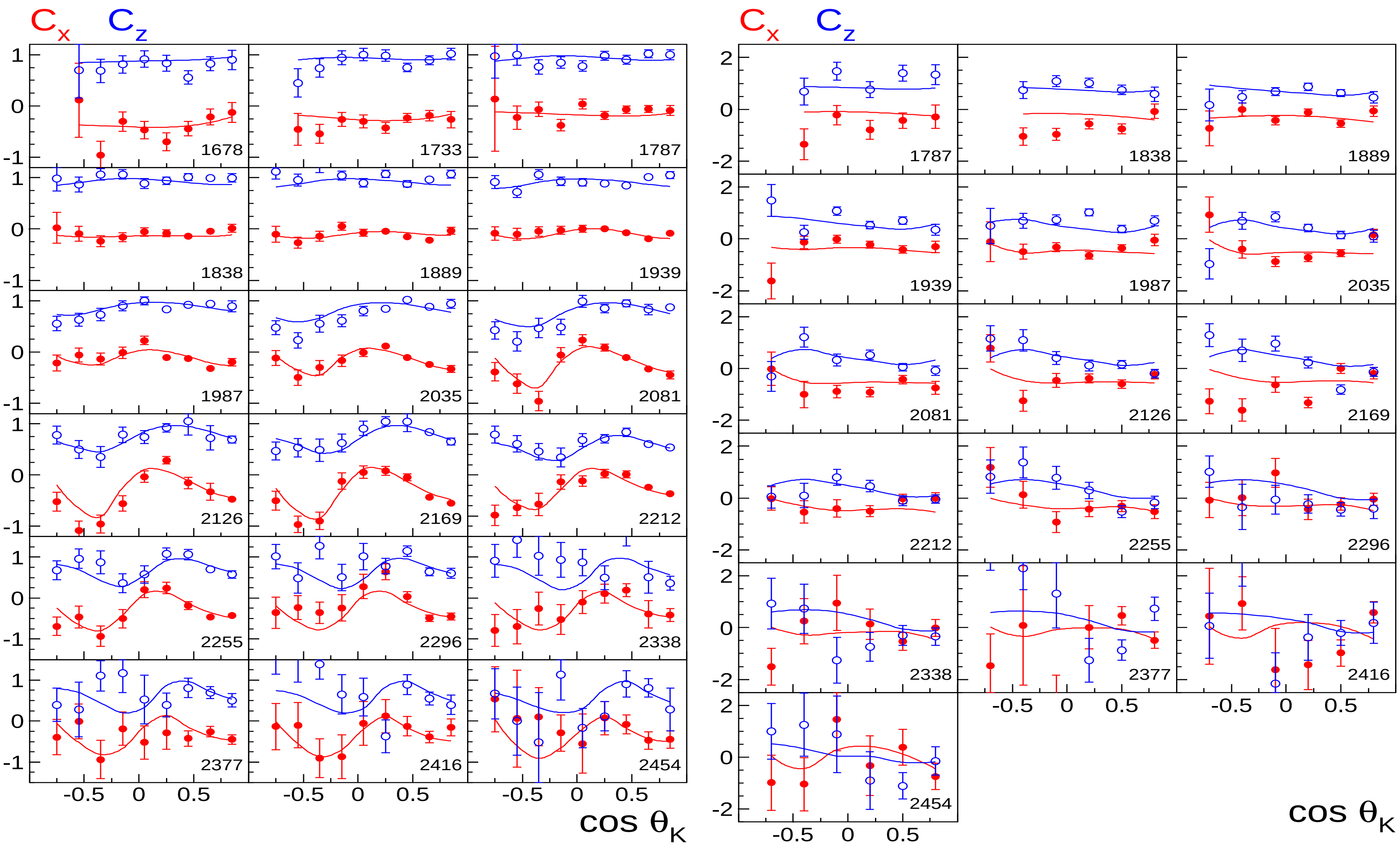

is supported by the new GRALL data on O_x O_z and T-observables: an important step to a complete experiment.

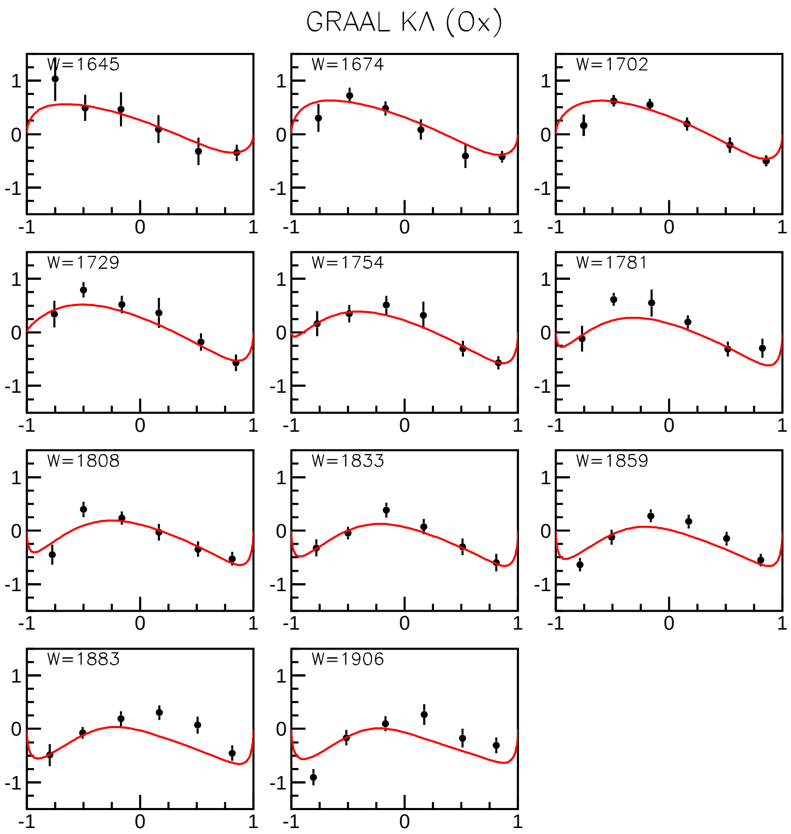

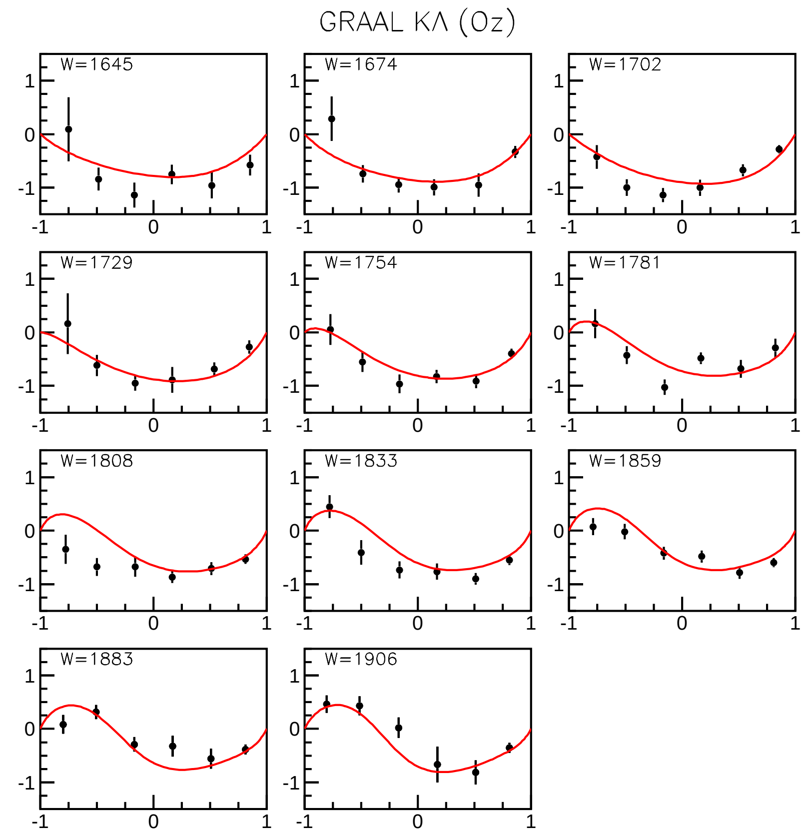

$\gamma p \to p\pi^0\eta$ (CB-ELSA)

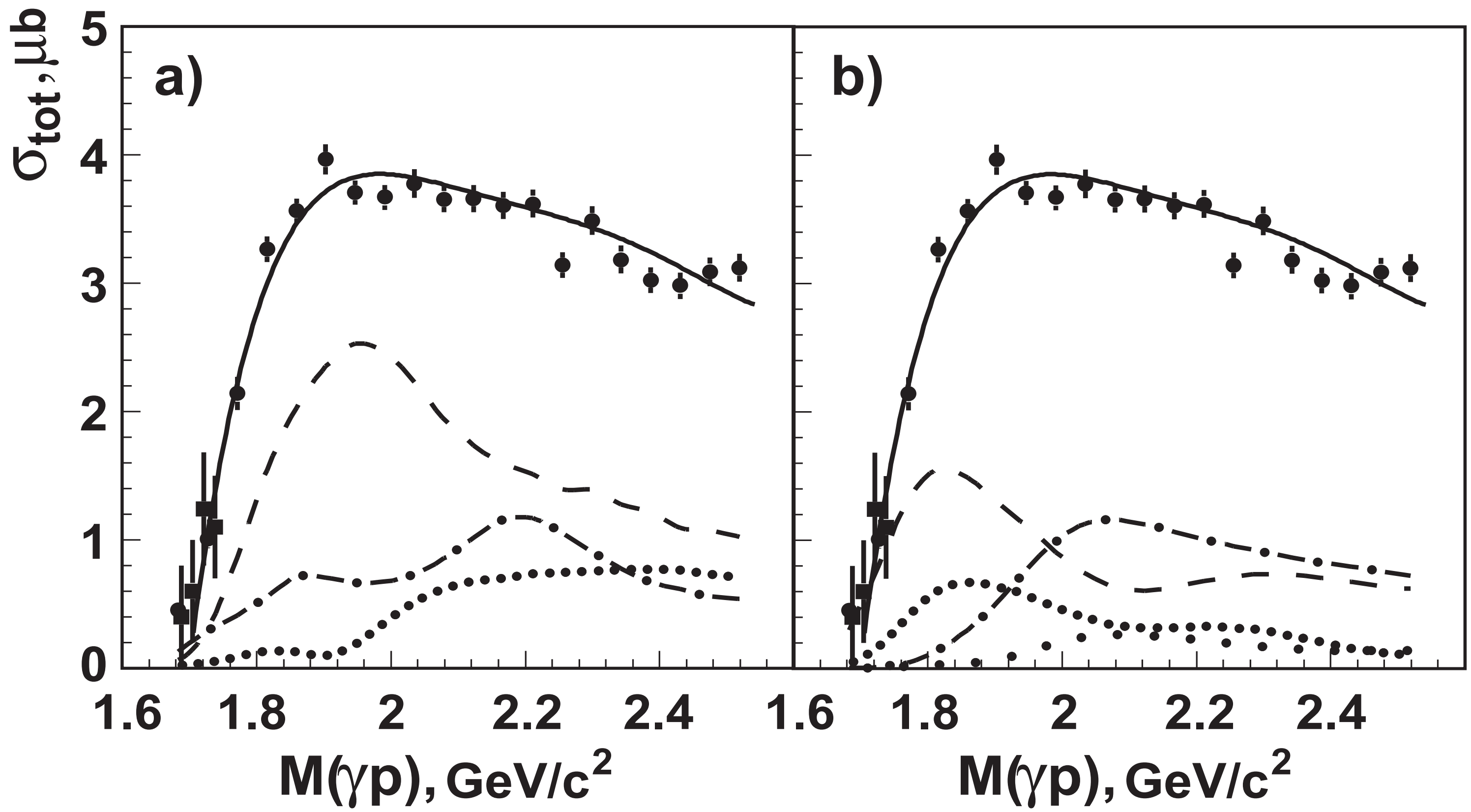

Left panel : contributions from $\Delta(1232)\eta$ (dashed), $S_{11}(1535)\pi$ (dashed-dotted) and $N\,a_0(980)$ final states.

Right panel: D_{33} partial wave (dashed), P_{33} partial wave (dashed-dotted), $D_{33} \to \Delta(1232)\eta$ (dotted) and $D_{33} \to N\,a_0(980)$ (wide dotted).

The $\gamma p \to \pi^0 \eta p$ differential cross section for the total energy region.

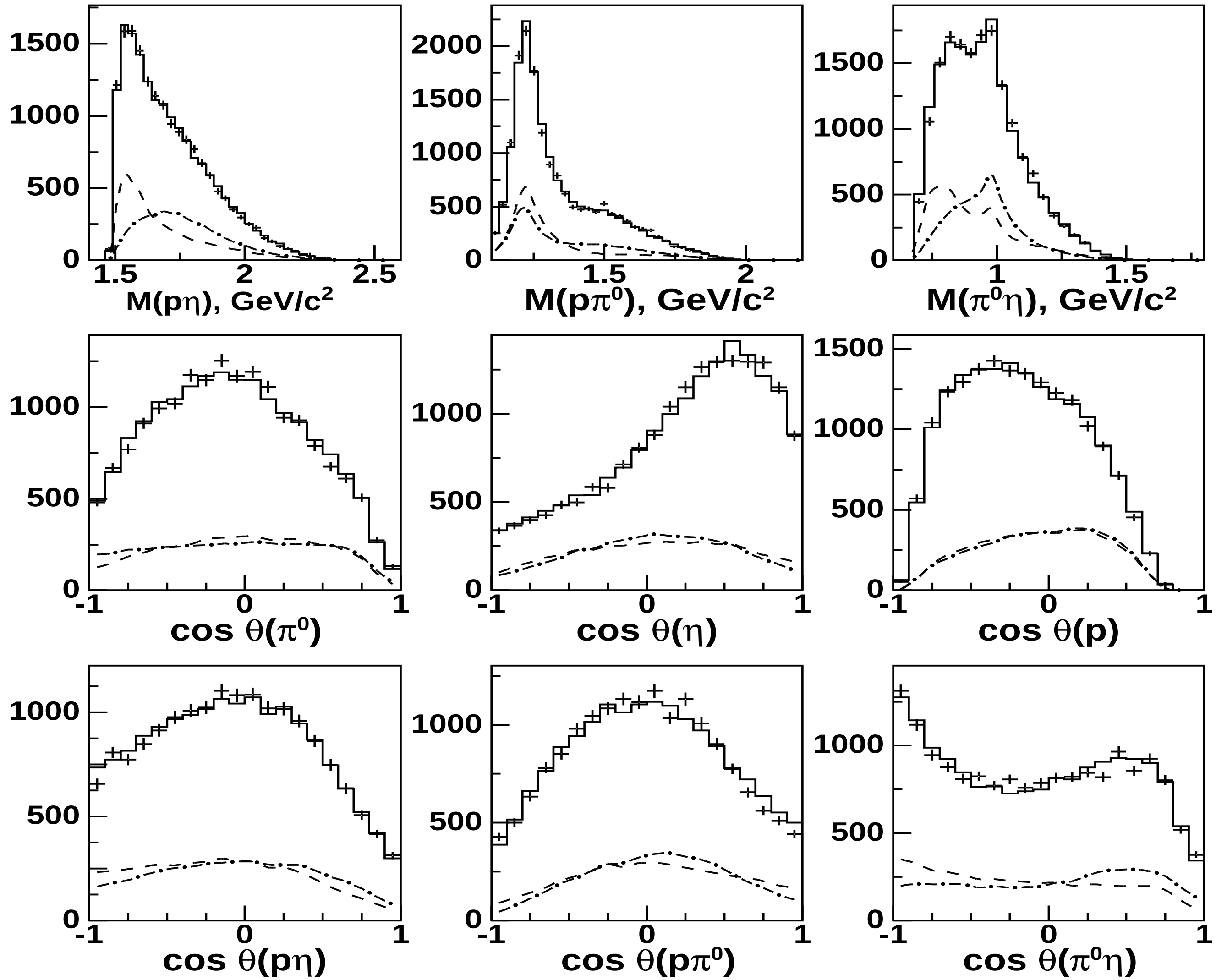

$N\pi \rightarrow N\pi\ D_{33}$ wave (3 pole 5 channel K-matrix)

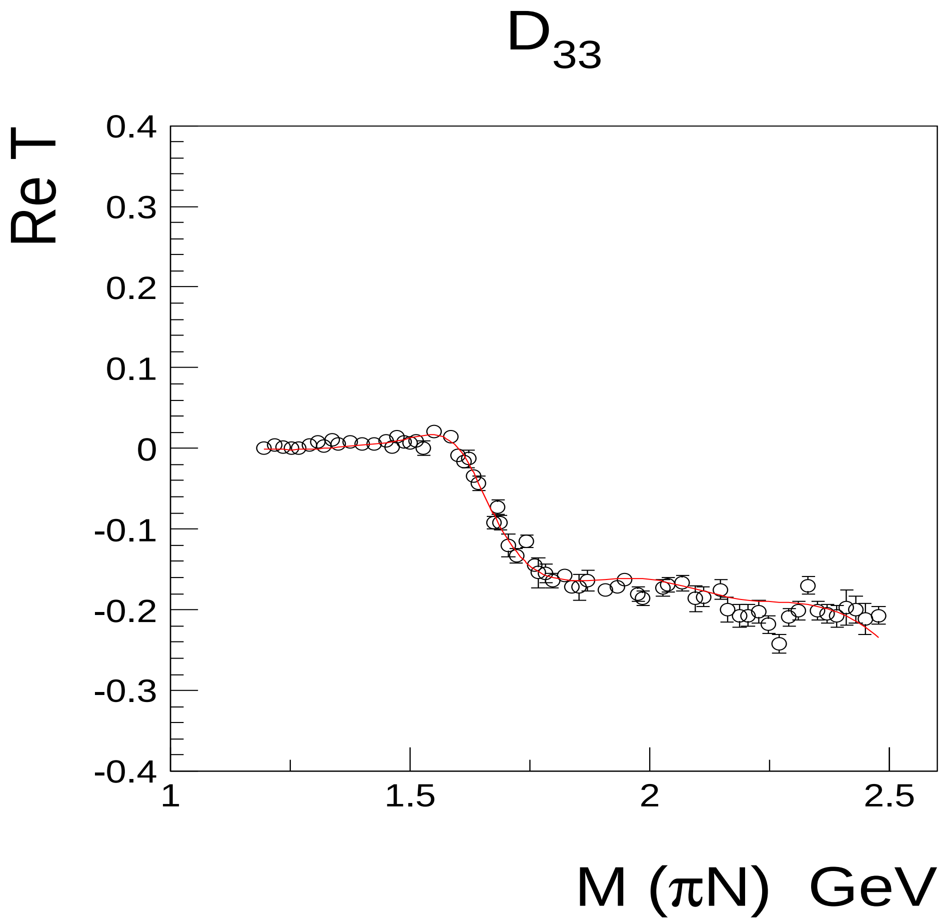

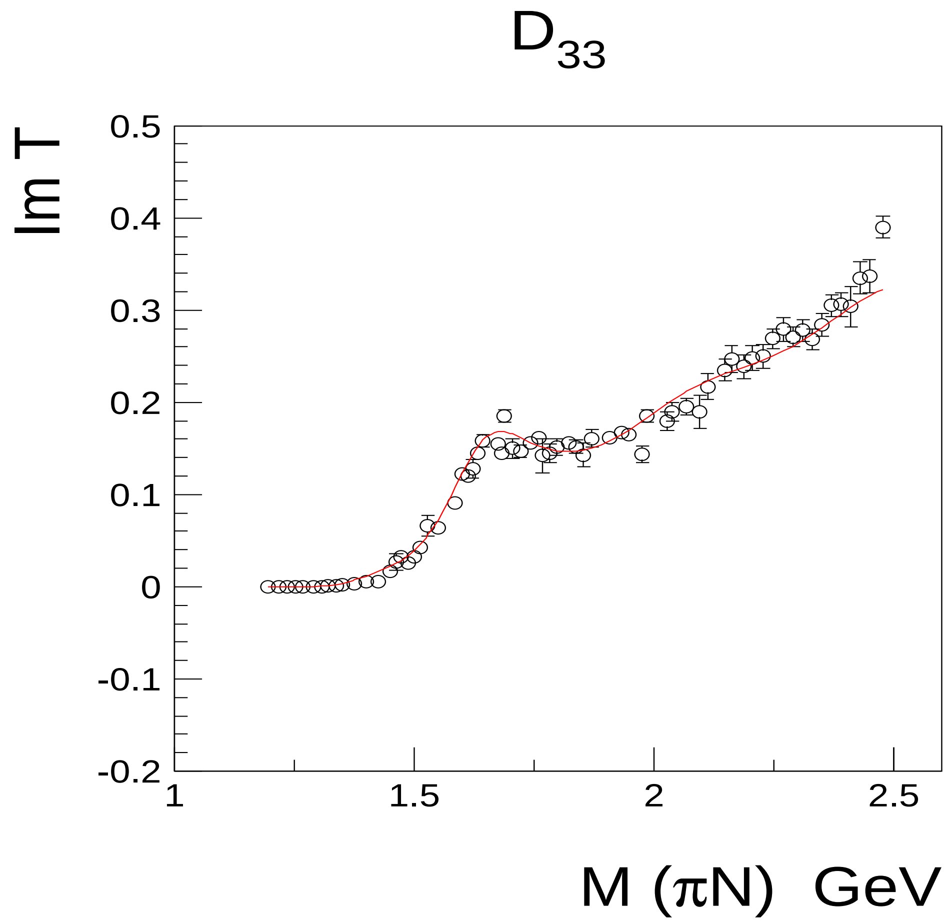

D_{33}**-wave:** πN, $\Delta(1232)\pi$ **(**S**- and** D**-waves)),** $\Delta(1232)\eta$, $S_{11}(1535)\pi$

Properties of the $\Delta(1920)P_{33}$ and $\Delta(1940)D_{33}$ resonances.

	M_{pole}	Γ_{pole}	M_{BW}	Γ_{tot}^{BW}
$\Delta(1920)P_{33}$	1980^{+25}_{-45}	350^{+35}_{-55}	1990 ± 35	375 ± 50
$\Delta(1940)D_{33}$	1985 ± 30	390 ± 50	1990 ± 40	410 ± 70

	$\mathrm{Br}_{N\pi}$	$\mathrm{Br}_{\Delta\eta}$	$\mathrm{Br}_{N(1535)\pi}$	$\mathrm{Br}_{Na_0(980)}$
$\Delta(1920)P_{33}$	15 ± 8	18 ± 8	7 ± 4	4 ± 2
$\Delta(1940)D_{33}$	9 ± 4	5 ± 2	2 ± 1	2 ± 1

Mass scan of P_{33} and D_{33} pole position

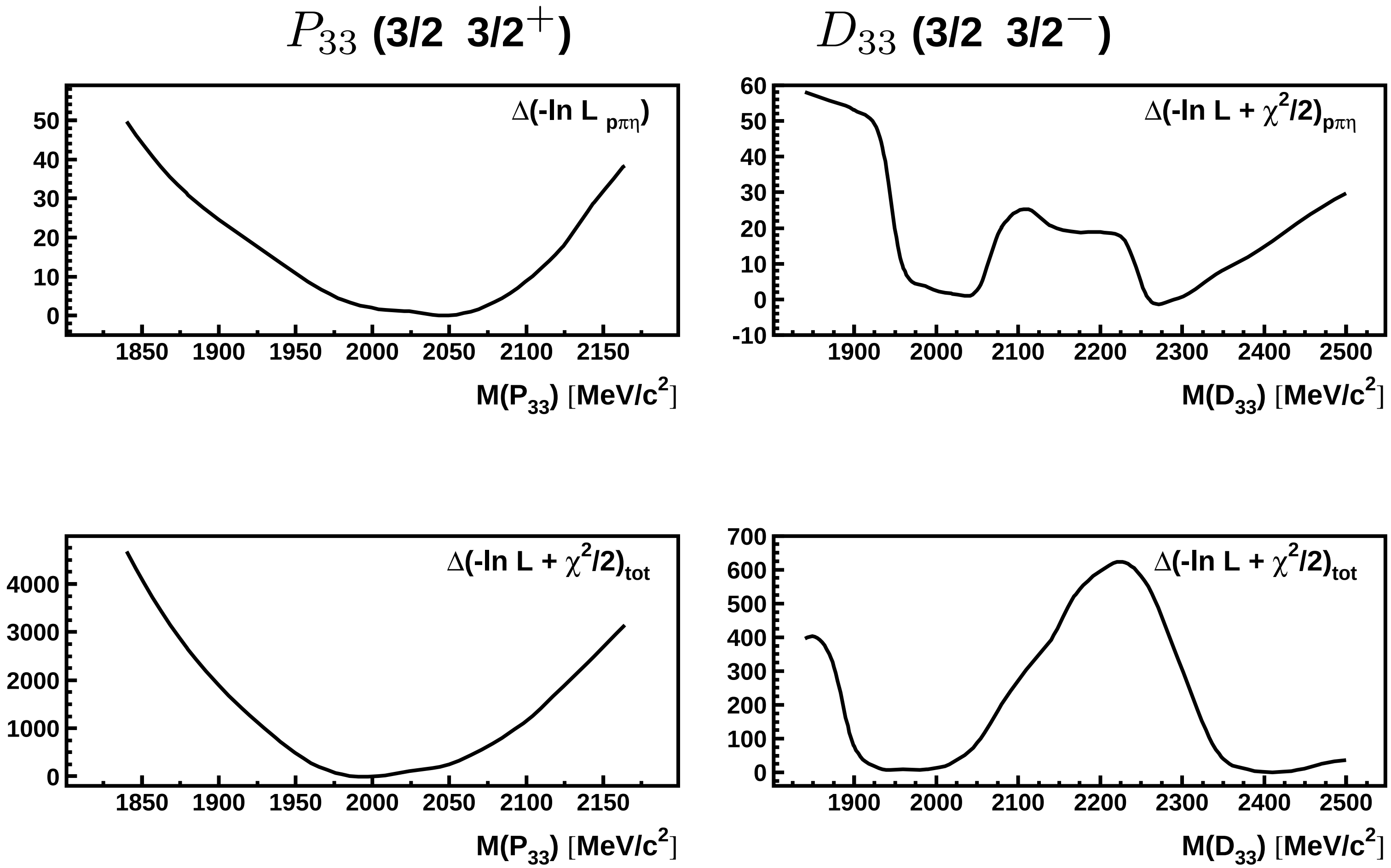

Parity doublets of N and Δ resonances at high mass region

Glozman suggested a restoration of chiral symmetry in high-mass excitations. Parity doublets must not interact by pion emission and could have a small coupling to πN.

$J=\frac{1}{2}$	$N_{1/2+}(2100)^a$	*	$N_{1/2-}(2090)^a$	*	$\Delta_{1/2+}(1910)$	****	$\Delta_{1/2-}(1900)^a$	**
$J=\frac{3}{2}$	$N_{3/2+}(1900)^a$	**	$N_{3/2-}(2080)^a$	**	$\Delta_{3/2+}(1920)^a$	***	$\Delta_{3/2-}(1940)^a$	*
$J=\frac{5}{2}$	$N_{5/2+}(2000)^a$	**	$N_{5/2-}(2200)^a$	**	$\Delta_{5/2+}(1905)$	****	$\Delta_{5/2-}(1930)^a$	***
$J=\frac{7}{2}$	$N_{7/2+}(1990)^a$	**	$N_{7/2-}(2190)$	****	$\Delta_{7/2+}(1950)$	****	$\Delta_{7/2-}(2200)^a$	*
$J=\frac{9}{2}$	$N_{9/2+}(2220)$	****	$N_{9/2-}(2250)$	****	$\Delta_{9/2+}(2300)$	**	$\Delta_{9/2-}(2400)^a$	**

$J=\frac{3}{2}$	$N_{3/2+}(1900)$	$N_{3/2-}(1875)$	$\Delta_{3/2+}(1980)$	$\Delta_{3/2-}(1985)$
$J=\frac{5}{2}$	$N_{5/2+}(1960)$	$N_{5/2-}(2070)$	$\Delta_{5/2+}(1945)$	$\Delta_{5/2-}(1930)$
$J=\frac{7}{2}$	$N_{7/2+}(1990)$	$N_{7/2-}(????)$	$\Delta_{7/2+}(1910)$	$\Delta_{7/2-}(????)$

Holographic QCD (AdS/QCD)

Soft-wall model prediction: $M^2_{N,L} = 4\lambda^2 \left(N + L + \frac{3}{2}\right)$

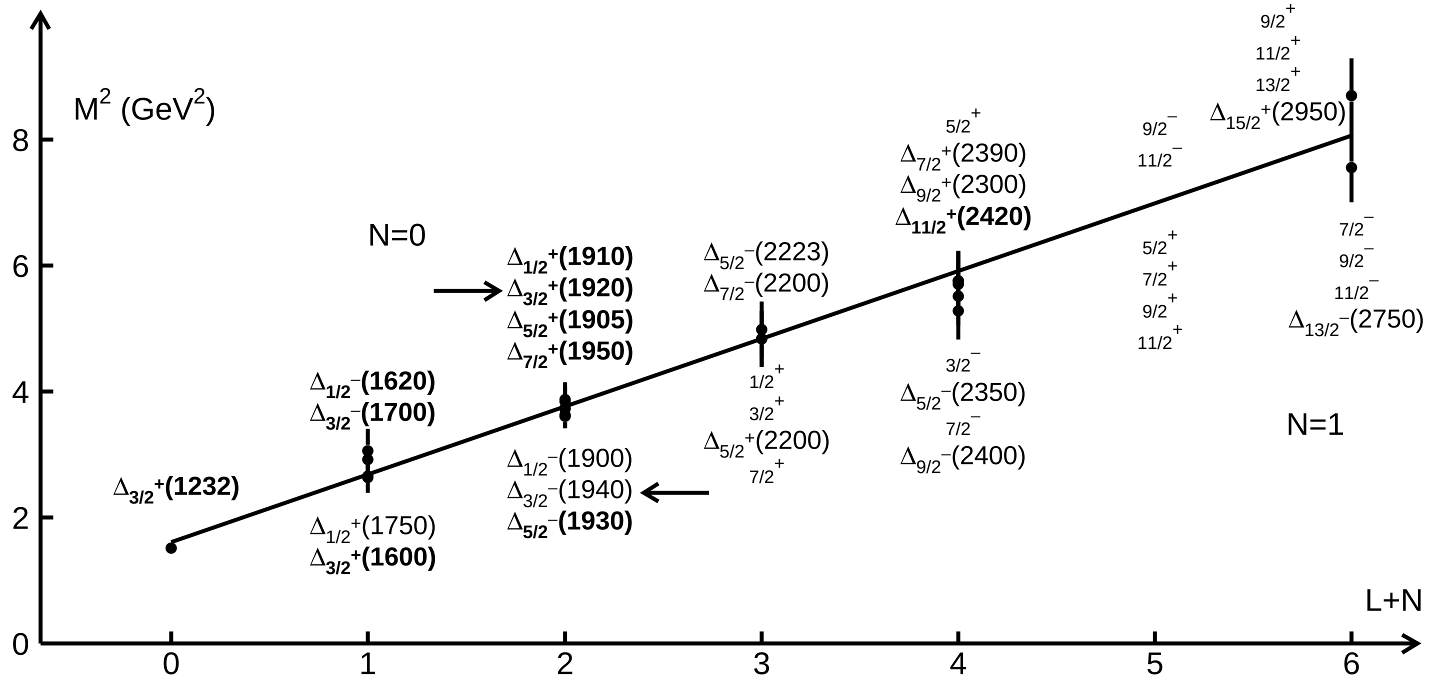

$$M^2_{N,L} = 4\lambda^2 \left(N + L + \frac{3}{2}\right) - 2\left(M^2_\Delta - M^2_N\right)\kappa_{gd}$$

κ_{gd} **is the fraction of most attractive color-antitriplet isosinglet diquark.**

κ_{gd}**=0 for** Δ **and N(S=3/2) states,** $\frac{1}{2}$ **for** $S = 1/2\ (70 SU_6)$ **and** $\frac{1}{4}$ **for** $S = 1/2\ (56 SU_6)$**.**

Hilmar Forkel and Eberhard Klempt, hep-ph:0810.2959v1

L, S, N	κ_{gd}	Resonance					Pred.
0,$\frac{1}{2}$,0	$\frac{1}{2}$	$N(940)$				input:	0.94
0,$\frac{3}{2}$,0	0	$\Delta(1232)$					1.27
0,$\frac{1}{2}$,1	$\frac{1}{2}$	$N(1440)$					1.40
1,$\frac{1}{2}$,0	$\frac{1}{4}$	$N(1535)$	$N(1520)$				1.53
1,$\frac{3}{2}$,0	0	$N(1650)$	$N(1700)$	$N(1675)$			1.64
1,$\frac{1}{2}$,0	0	$\Delta(1620)$	$\Delta(1700)$		L, S, N=0,$\frac{3}{2}$,1:	$\Delta(1600)$	1.64
2,$\frac{1}{2}$,0	$\frac{1}{2}$	$N(1720)$	$N(1680)$		L, S, N=0,$\frac{1}{2}$,2:	$N(1710)$	1.72
1,$\frac{1}{2}$,1	$\frac{1}{4}$	$N(????)$	$N(1875)$				1.82
1,$\frac{3}{2}$,1	0	$\Delta(1900)$	$\Delta(1940)$	$\Delta(1930)$			1.92
2,$\frac{3}{2}$,0	0	$\Delta(1910)$	$\Delta(1920)$	$\Delta(1905)$	$\Delta(1950)$		1.92
2,$\frac{3}{2}$,0	0	$N(1880)$	$N(1900)$	$N(1990)$	$N(2000)$		1.92
0,$\frac{1}{2}$,3	$\frac{1}{2}$	$N(2100)$					2.03
3,$\frac{1}{2}$,0	$\frac{1}{4}$	$N(2070)$	$N(2190)$	L, S, N=1,$\frac{1}{2}$,2:	$N(2080)$	$N(2090)$	2.12
3,$\frac{3}{2}$,0	0	$N(2200)$	$N(2250)$	L, S, N=1,$\frac{1}{2}$,2:	$\Delta(2223)$	$\Delta(2200)$	2.20
4,$\frac{1}{2}$,0	$\frac{1}{2}$	$N(2220)$					2.27
4,$\frac{3}{2}$,0	0	$\Delta(2390)$	$\Delta(2300)$	$\Delta(2420)$	L, N=3,1:	$\Delta(2400)$	2.43
5,$\frac{1}{2}$,0	$\frac{1}{4}$	$N(2600)$				$\Delta(2350)$	2.57

Search for baryon states in $\gamma p \to p\pi^0\pi^0$ (3.2 GeV)

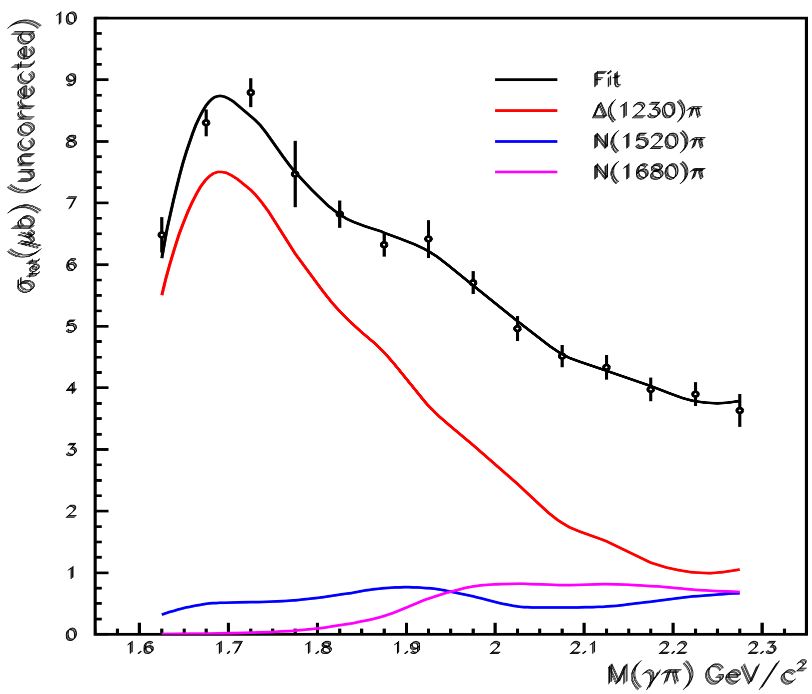

Mass and angular projections.

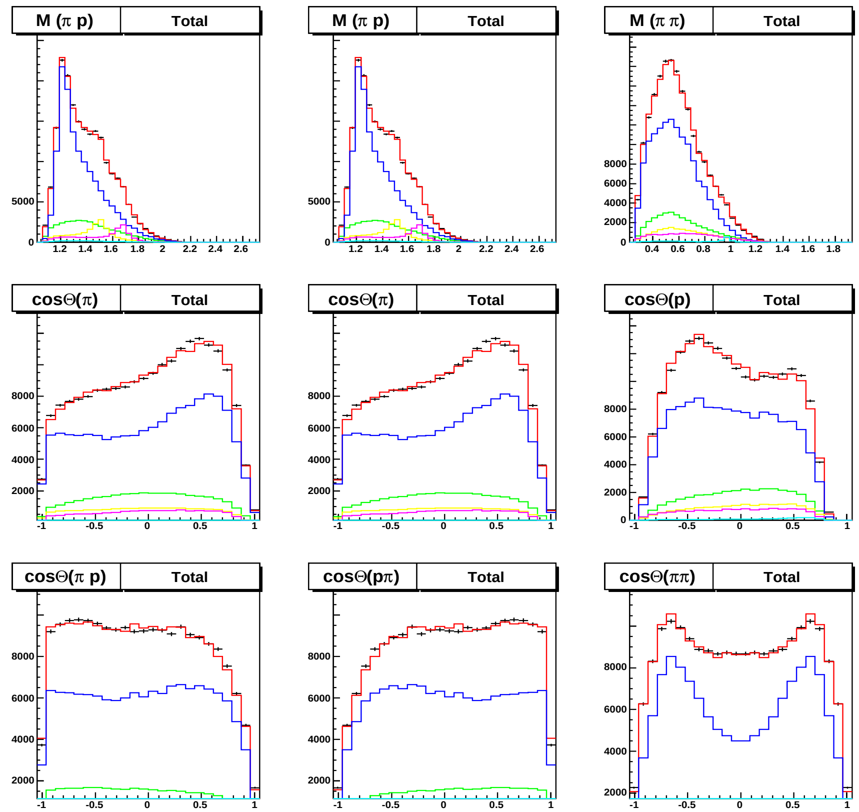

A preliminary analysis reveals only one (relatively) new state:

$S_{31}(1900)$ **with** $M \sim 2010$ **MeV and** $\Gamma \sim 430 MeV$

Polarization information is urgently needed.

η-photoproduction at the neutron - CB-ELSA/TAPS data -

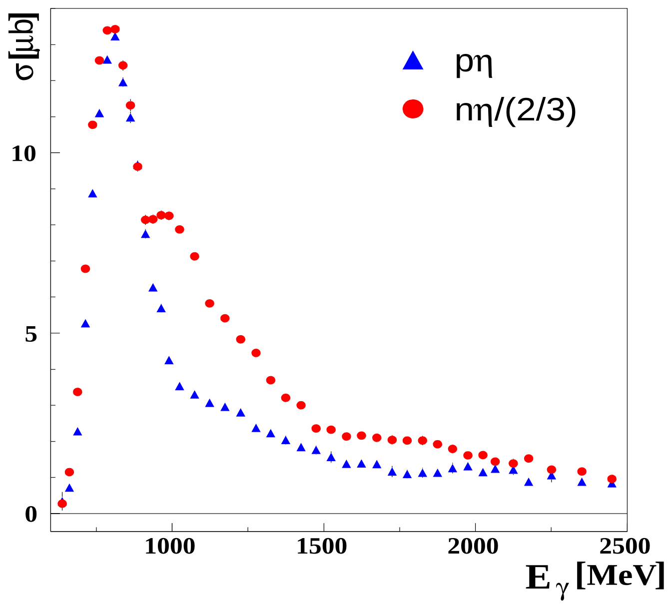

Investigation of $\gamma d \rightarrow n\eta\ (p);\ \eta \rightarrow 3\pi^0$

$\leftrightarrow$ also CB-ELSA/TAPS data shows an enhancement around 1670 MeV (preliminary)

σ_n/σ_p $\Rightarrow$
data in comparison to MAID (—) prediction
$\leftrightarrow$ effect of the $D_{15}(1675)$

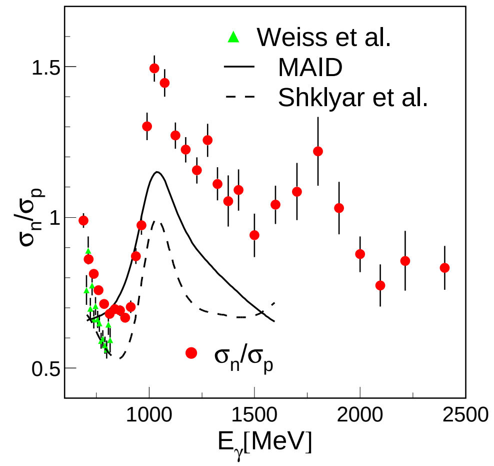

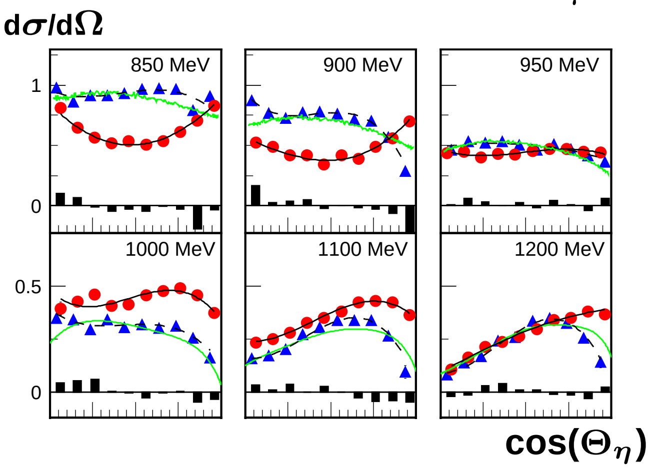

$\leftrightarrow$ something quite interesting going on

- **role of the $D_{15}(1675)$?**
- **narrow $P_{11}(1670)$?**
- **explainable by S_{11}-states + $P_{11}(1710)$?**
- **interference of $S_{11}(1535)/S_{11}(1650)$?**

$\leftrightarrow$ additional observables needed

Three different class of solutions are found:

1. **solutions with strong interference in S_{11} wave;**
2. **solutions with $N(1710)P_{11}$ resonance;**
3. **solutions with narrow state in the mass region 1665 MeV.**

Observable	N_{data}	$\frac{\chi^2}{N_{\mathrm{data}}}$ Sol. 1	$\frac{\chi^2}{N_{\mathrm{data}}}$ Sol. 2	$\frac{\chi^2}{N_{\mathrm{data}}}$ Sol. 3	Ref.
$\sigma(\gamma \mathrm{n} \to \mathrm{n}\eta)$	280	1.32	1.37	1.31	CB-ELSA
$\Sigma(\gamma \mathrm{n} \to \mathrm{n}\eta)$	88	1.75	2.07	1.79	GRAAL
$\sigma(\gamma \mathrm{n} \to \mathrm{n}\pi^0)$	147	2.01	2.48	2.03	SAID database
$\Sigma(\gamma \mathrm{n} \to \mathrm{n}\pi^0)$	28	1.02	0.95	0.90	GRAAL

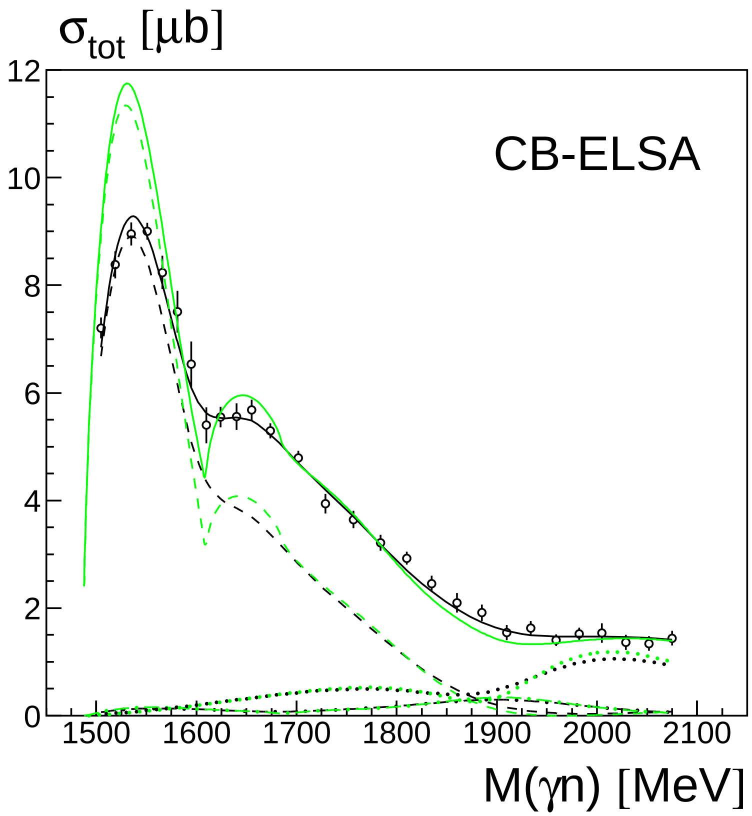

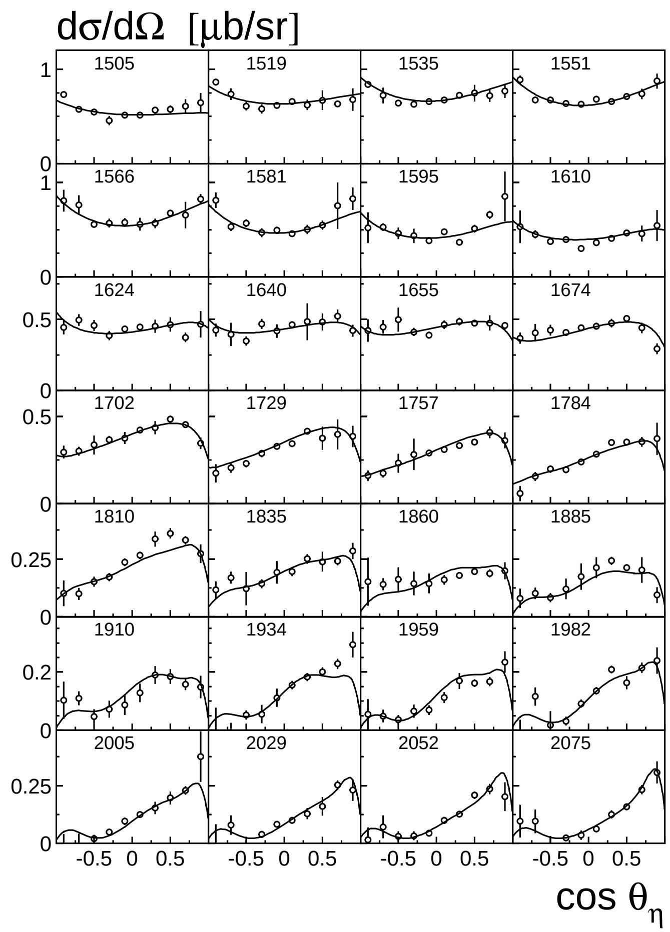

The total and differential cross section for the reaction $\gamma n \to \eta n$ obtained on the deuteron target. The PWA result from the solution with S_{11} interference (solution 1) is shown. The green curves show the corresponding cross sections on the free neutron target (no Fermi motion). Contributions: S_{11} (dashed), P_{13} (dotted) and P_{11} (dash-dotted)

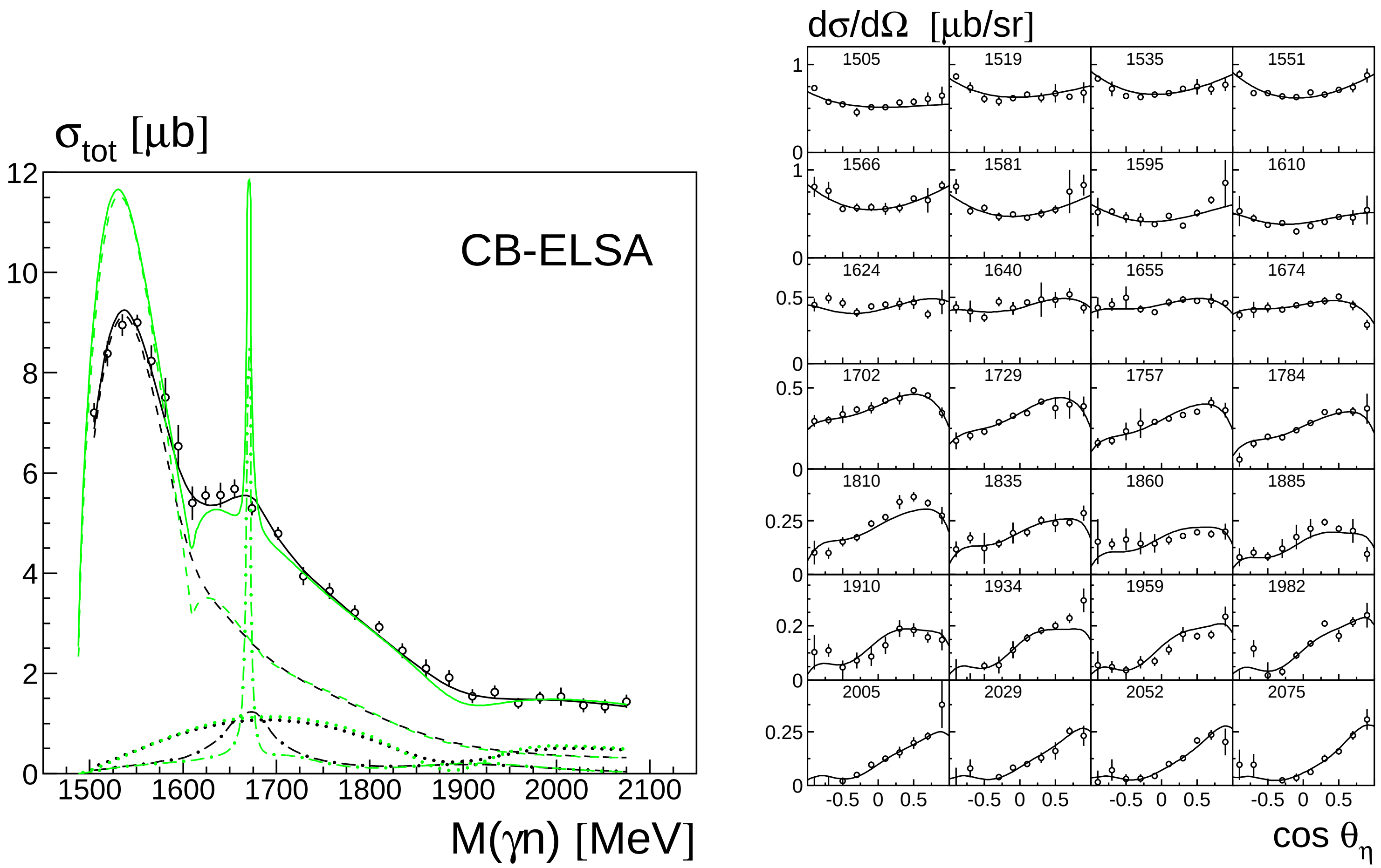

The total and differential cross section for the reaction $\gamma \mathrm{n} \to \eta \mathrm{n}$ obtained on the deuteron target. The PWA result from the solution with narrow P_{11} resonance (solution 3) is shown. The green curves show the corresponding cross sections on the free neutron target (no Fermi motion). Contributions: S_{11} (dashed), P_{13} (dotted) and P_{11} (dash-dotted)

Beam asymmetry for the $\gamma n \to \eta n$ and $\gamma n \to \pi^0 n$

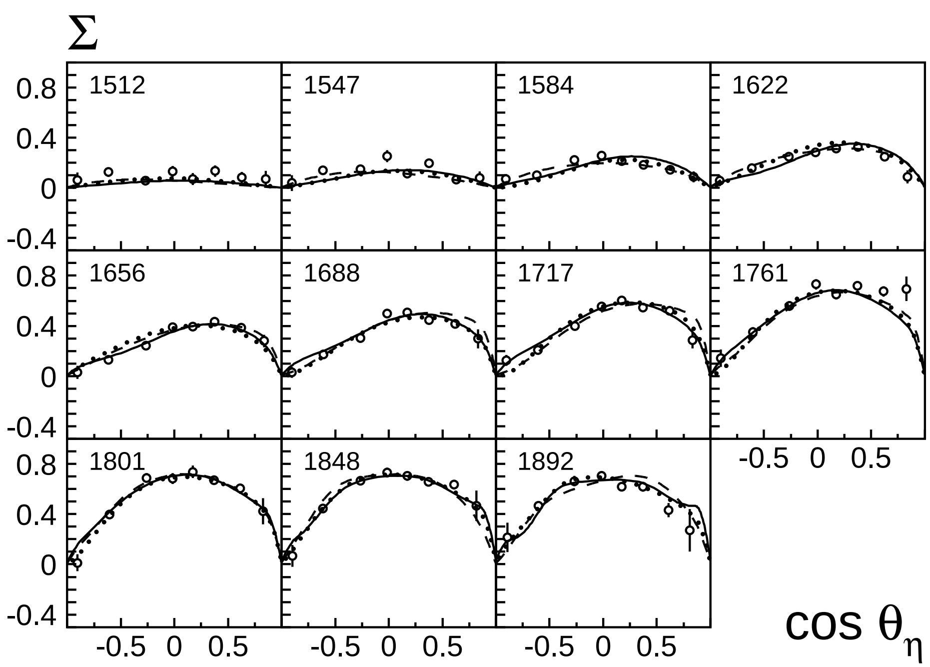

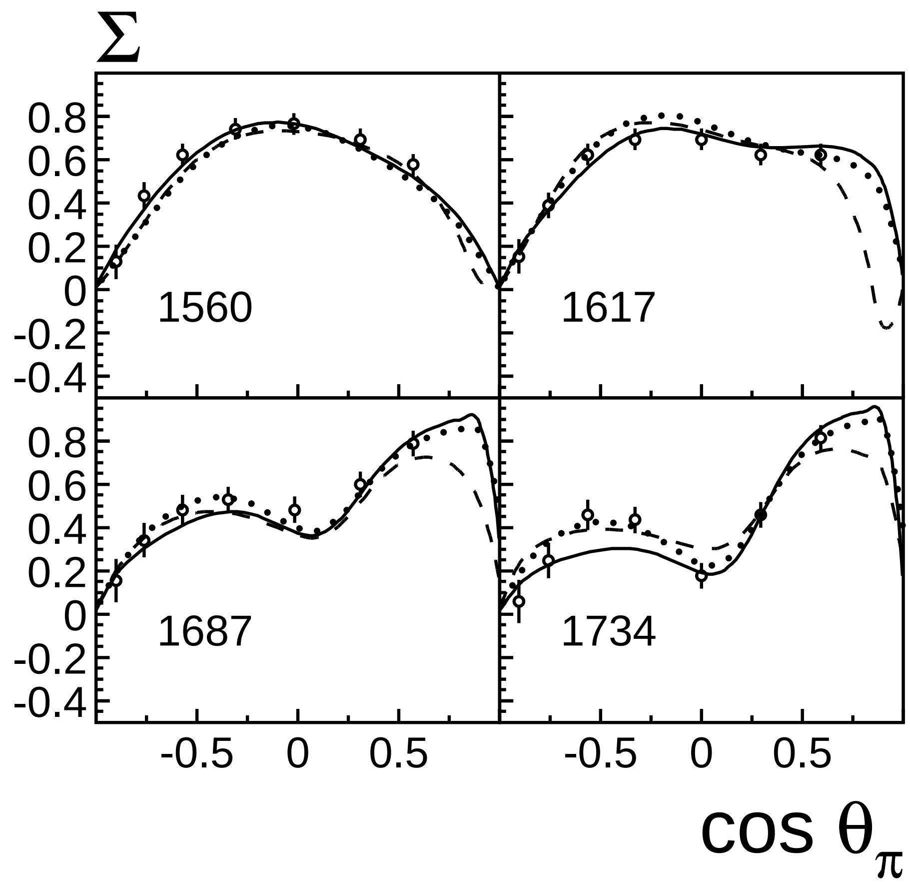

Beam asymmetry for the $\gamma p \rightarrow \eta p$ with fine bins

Solution 1: $\chi^2 = 1.35$ **Solution 3:** $\chi^2 = 0.95$

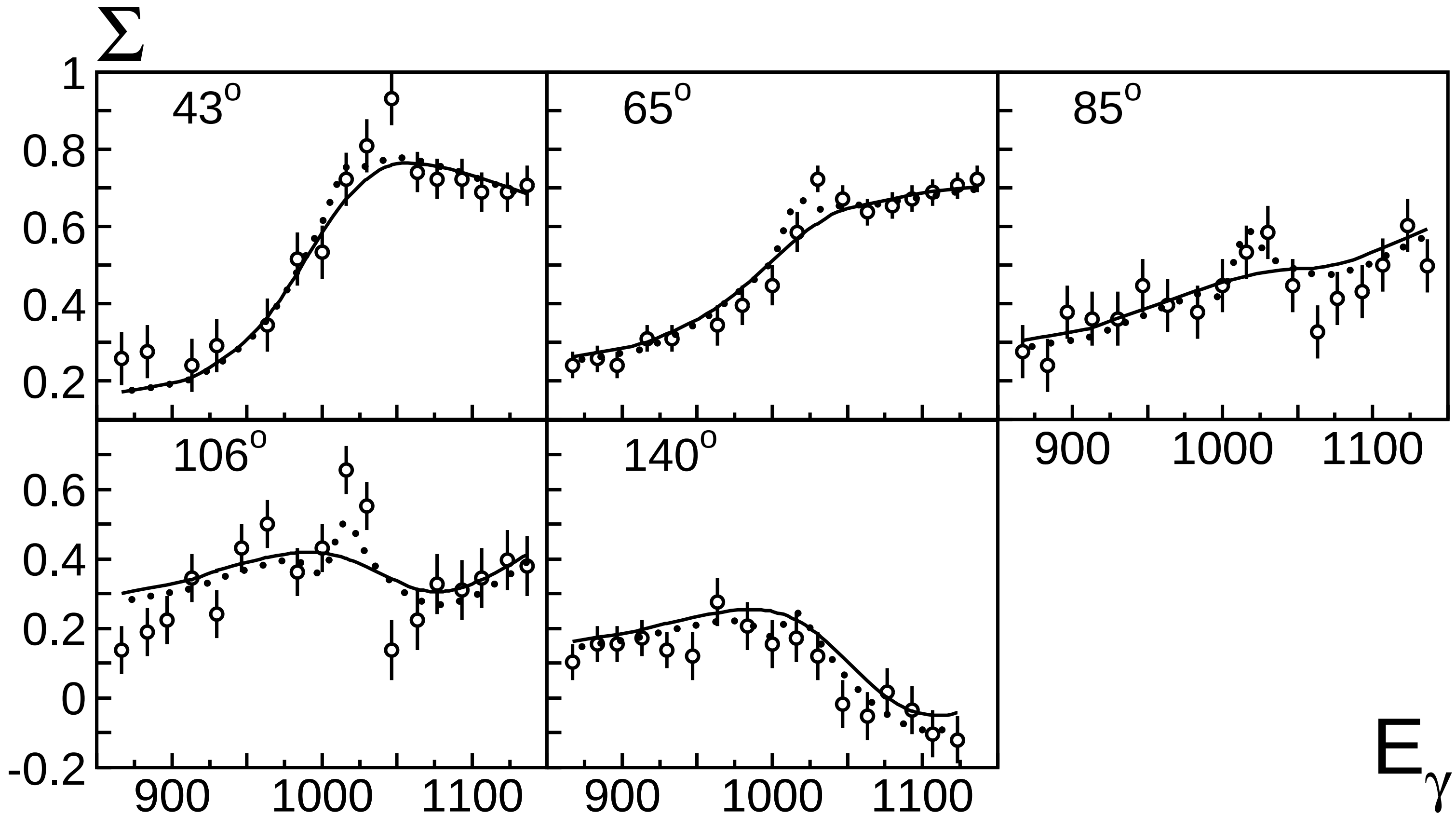

The long-standing discrepancies between the photo-production amplitude $A^n_{1/2}$ for $N(1535)S_{11}$ production ($A^n_{1/2} = -0.020 \pm 0.035$ GeV$^{-1/2}$ from $\gamma n \to n\pi^0$ (Arndt); $A^n_{1/2} = -0.100 \pm 0.030$ GeV$^{-1/2}$ from $\gamma n \to n\eta$ (Krusche) is solved.

	$S_{11}(1535)$	$S_{11}(1650)$
Pole position (mass)	1.505 ± 0.020	1.640 ± 0.015
(width)	0.145 ± 0.025	0.165 ± 0.015
PDG	1.510 ± 0.020	1.655 ± 0.015
	0.170 ± 0.080	0.165 ± 0.015
$A^p_{1/2}$ **(GeV$^{-1/2}$)**	0.090 ± 0.025	0.100 ± 0.035
PDG	0.090 ± 0.030	0.053 ± 0.016
phase	$(20 \pm 15)^\circ$	$(25 \pm 20)^\circ$
$A^n_{1/2}$ **(GeV$^{-1/2}$)**	-0.080 ± 0.020	-0.055 ± 0.020
PDG	-0.046 ± 0.027	-0.015 ± 0.021
phase	$(20 \pm 20)^\circ$	$(30 \pm 25)^\circ$

Summary

1. **An approach for the combined analysis of the pion and photo induced reaction with two and multi particle final states is developed.**
2. **The combined analysis of more them 65 different reactions helped to identify the properties of known baryons.**
3. **The new data support the two new baryon states observed in hyperon photoproduction $P_{11}(1880)$ and $P_{13}(1900)$.**
4. **The η-photoproduction data reveal the baryon resonance $D_{15}(2070)$.**
5. **The $D_{33}(1940)$ state is needed for the description of the $\gamma p \to \pi^0 \eta p$ data.**
6. **The structure at 1670 MeV observed in the η photoproduction data off neutron can be explained either by the interference within S_{11} wave or by a contribution of a narrow P_{11} state with mass 1670 ± 6 MeV.**
7. **The spectrum of observed states is in direct contradiction with a classical quark model. The best explanations are chiral symmetry restoration or AdS/QCD soft-wall model.**